18th International Conference on Space Operations, Montreal, Canada, 26 - 30 May 2025.


SpaceOps-2025, ID # 227

# JWST Fine Guidance Sensor Commissioning and Performance During Operations

M. Begoña Vila*[b,a], Bruce Barringer[d], Nicholas Bond[g,a], Pierre Chayer[d], Audrey DiFelice[d], Jean Dupuis[f], Sherie Holfeltz[d], Scott D. Lambros[c,a], Amanda Marrione[d], Christopher D. Moller[c,a], Ed Nelan[d], Neil Rowlands[e], S. Tony Sohn[d], Gerald Warner[e], Jared Yeates[e], Julia Zhou[f].

[a]NASA's Goddard Space Flight Center, 8800 Greenbelt Rd, Greenbelt, MD 20771

[b]KBR, 7701 Greenbelt Rd #400, Greenbelt, MD 20770

[c]Aerodyne Industries, 7701 Greenbelt Road, Suite 300, Greenbelt, Md. 20770

[d]Space Telescope Science Institute, 3700 San Martin Dr, Baltimore, MD 21218

[e]Honeywell Aerospace, 400 Maple Grove Rd, Kanata, ON, Canada K2V 1B8

[f]Canadian Space Agency/Agence Spatiale Canadienne, 6767 Rte de l'Aéroport, Saint-Hubert, QC J3Y, 8Y9, Canada

[g]Adnet Systems Inc, 6720B Rockledge Dr #504, Bethesda, MD 20817

**ABSTRACT**

The Fine Guidance Sensor (FGS) Instrument on the James Webb Space Telescope (JWST) provides accurate Guide Star information every 64 ms to the Attitude Control System (ACS) to maintain the pointing stability needed for science operations. This involves identifying and tracking the correct Guide Star in different types of astrometrical fields and it is run as an event driven operation working through the different guider modes (Identification, Acquisition, Track and Fine Guide) with interleaved slews and operations with the Attitude Control System. This paper summarizes activities undertaken during the Commissioning period, including guiding with different Point Spread Functions (PSFs) as the JWST mirrors were being aligned and focused, and instances in which the Guide Stars selected by the Guide Star Catalogue had to be updated to match what was expected to be imaged on the FGS detector based on the mirror's state. A significant amount of ground testing with simulated images was required in order to prepare for on orbit operations. This paper also covers several calibrations and optimizations completed during this period.

The current normal operations performance is also presented. For normal operations there are sparse fields, bright crowded fields and Guide Stars of different brightnesses which require different accommodations. JWST also observes nearby objects in the solar system that require a different 'moving target' mode for guiding. Bad pixel maps need to be updated at a regular cadence. Performance to date exceeds requirements with typical pointing stability of ~ 1 mas. The information from FGS is also used to identify updates needed in the Guide Star Catalogue by identifying photometric inaccuracies, duplicate Guide Star entries, misclassified objects (e.g. classified as stars but are actually galaxies), etc.

A continuous improvement operational concept has evolved which identifies unsuccessful Visits to understand the reason behind any performance issues (whether they are attributable to FGS parameters/algorithms, ACS pointing errors, Guide Star Catalogue errors, or something else). Visits which needed retries and Visits with high Noise Equivalent Angle are also studied and mitigation approaches have been implemented. The current success rate for finding and guiding on the correct commanded Guide Star is ~ 96%.

**Keywords:** Fine Guidance Sensor, Fine Guiding, Operational Scenarios, James Webb Space Telescope, Guide Star Identification, Guide Star Acquisition.

**Acronyms**

ACQ - Acquisition
ACS – Attitude Control System
BCF – Bright Crowded Field
BPM – Bad Pixel Map
CSA – Canadian Space Agency
FG – Fine Guide
FGC – Fine Guidance Control
FGS – Fine Guidance Sensor
FOV – Field of View
FSM – Fine Steering Mirror
FSW – Flight Software
GS – Guide Star
GSC – Guide Star Catalogue
GSFC – Goddard Space Flight Center
GSSS – Guide Star Selection System
HGA – High Gain Antenna
ID - Identification
JWST – James Webb Space Telescope
MIRI – Mid-Infrared Instrument
MSA – Micro-Shutter Array
MT – Moving Target
NEA – Noise Equivalent Angle
NIRCam – Near Infrared Camera
NIRISS – Near Infrared Imager and Slitless Spectrograph
NIRSpec – Near Infrared Spectrograph
OSS – Operations Script Subsystem
OTE – Optical Telescope Element
PSF – Point Spread Function
RS – Reference Star
SAM – Small Angle Maneuver
SI – Science Instrument
STScI – Space Telescope Science Institute
TRK - Track

## 1. Introduction

The James Webb Space Telescope (JWST) is the next premier space infrared telescope which looks back in time to the first galaxies and stars that were formed 13.5 billion years ago, studies star and galaxy formation, and identifies exoplanets and their constituent components. The Observatory is composed of a 6.5 m diameter, segmented, deployable primary mirror, an Integrated Science Instrument Module (ISIM), a deployable tennis-court sized sunshield, and a spacecraft element for communications, control and other housekeeping functions. JWST was launched on December 25, 2021.

The primary mirror is made up of 18 individual hexagonal mirror segments which fold up to fit in the launch vehicle, are aligned to appear as one primary mirror, and have diffraction limited performance at a wavelength of 2 µm. The ISIM consists of four Science Instruments (SI) and a guider, and various structural, thermal, electronic, and operational systems that support them. The instruments are a Near Infrared Camera (NIRCam), a Near Infrared Spectrograph (NIRSpec), a Mid-Infrared Instrument (MIRI), and a Fine Guidance Sensor/Near Infrared Imager and

Slitless Spectrograph (FGS/NIRISS) [1, 2]. Together they encompass the wavelength range of 0.5 – 28 μm giving an unprecedented view of the Universe at those wavelengths. The instruments are a contribution from partners in Europe, Canada and the US. See Gardner et al. [3] on the JWST Mission and Rigby et al. [4] for a summary of the JWST Performance post commissioning.

For scientific observations a required milli-arcsec pointing accuracy and stability is achieved by the Fine Guidance Controller which includes the Fine Guidance Sensor instrument (FGS), the Attitude Control System (ACS), and the Fine Steering Mirror (FSM).

The Fine Guidance Sensor contains two separate detector channels, sensitive over a broad passband of 0.5 μm to 5.0 μm, called Guider 1 and Guider 2 (for redundancy and greater accuracy) to provide, as the name implies, pointing error signals on selected Guide Stars to the Attitude Control System for high precision fine pointing and stability of the Observatory. FGS provides source positions of the Guide Stars (GS) (centroids) along with quality indicators every 64 ms, to an accuracy of better than 4 milli-arcsecs, typically 1 milli-arcsec. GS magnitudes range from bright limit of J =12.5 to a faint limit of J=17.8. Together, the combined areal coverage of the sky by Guider 1 and Guider 2 is 10.9 amin$^2$, which assures that at least one catalogued Guide Star suitable for guiding is available with a better than 95% probability anywhere on the sky.

This paper summarizes the fine guiding activities during the commissioning period, initially while the segmented mirror was being aligned and the optimizations identified for normal operations. It also provides information on the current performance that is approximately 96% in success rate finding the correct Guide Star and thus enabling successful science with the other science instruments.

## 2. Guiding with the JWST Fine Guidance Sensor

### *2.1 Achieving Closed Loop (Fine Guidance Control)*

The Fine Guidance Control (FGC) closed loop guiding on JWST FGS is achieved by a handshake of various components commanded through the Operations Script Subsystem (OSS) that is comprised of on-board scripts that interface with the ACS flight software (FSW) and the FGS FSW and then once the closed loop is achieved, with the Science Instruments' (SIs) FSW for gathering science data. Once a science target is identified for one of the instruments the Guide Star Catalogue (GSC) is used to select suitable Guide Stars for either Guider 1 or Guider 2 and if possible to select nearby Reference Stars to aid the identification of the selected Guide Star. This information as well as other details needed for the on-board operations and science observations is loaded as a visit file. The information in that visit file is provided by OSS to the FGS FSW and includes the expected location and brightness of the visit's Guide Star and its uncertainty on the brightness and similar information for the associated Reference Stars (to be used by the FGS Identification or "ID" function) in the selected guider channel.

The flow to achieve closed loop guiding is captured pictorially in Figure 1, and is as follows: an initial slew from ACS to the desired sky location (ID attitude); once that slew has settled to the expected rate, OSS will command FGS to run its Identification (ID) function on the selected guider; if ID is successful OSS will command FGS to run its Acquisition (ACQ) function and find the Guide Star; if ACQ is successful OSS provides the information on where the GS was found to ACS for it to do a Small Angle Maneuver (SAM) to the science attitude; once settled at the science attitude OSS will command FGS to run its ACQ function again and find the GS at the science location; if ACQ at the science location is successful OSS provides the information to ACS to perform a small SAM (called a zero degree SAM) to correct the location of the GS; once this is completed OSS will command FGS to run its Track (TRK) function

to find the GS and start sending centroids with the position of the GS to ACS that autonomously will start using the Fine Steering Mirror (FSM) to move the GS to its needed location – in parallel FGS will adjust the location of the track window read on the detector to keep the GS centered; when the GS is less than 50 mas from the location indicated in the visit file, ACS will declare the closed loop has been achieved and OSS will command FGS to transition to its Fine Guide (FG) mode where the GS position will be read in its smallest detector window size. FGS will continue to send centroids every 64 ms to ACS so ACS can adjust the FSM to keep the GS steady, and hence the Observatory field of view, in its needed location for science. Once the loop is declared settled OSS will move to set up the science instruments that will be used for that observation. FGS will continue in FG mode autonomously until commanded to stop and find a new GS for another visit. With pitch/yaw controlled by FGS GS centroids and roll about the GS controlled by star tracker assemblies and inertial rate units (i.e., gyros), the Observatory is precisely pointed and stabilized for the science observations. See Meza et al. [5] and Menzel et al. [6] for more information on the JWST pointing control.

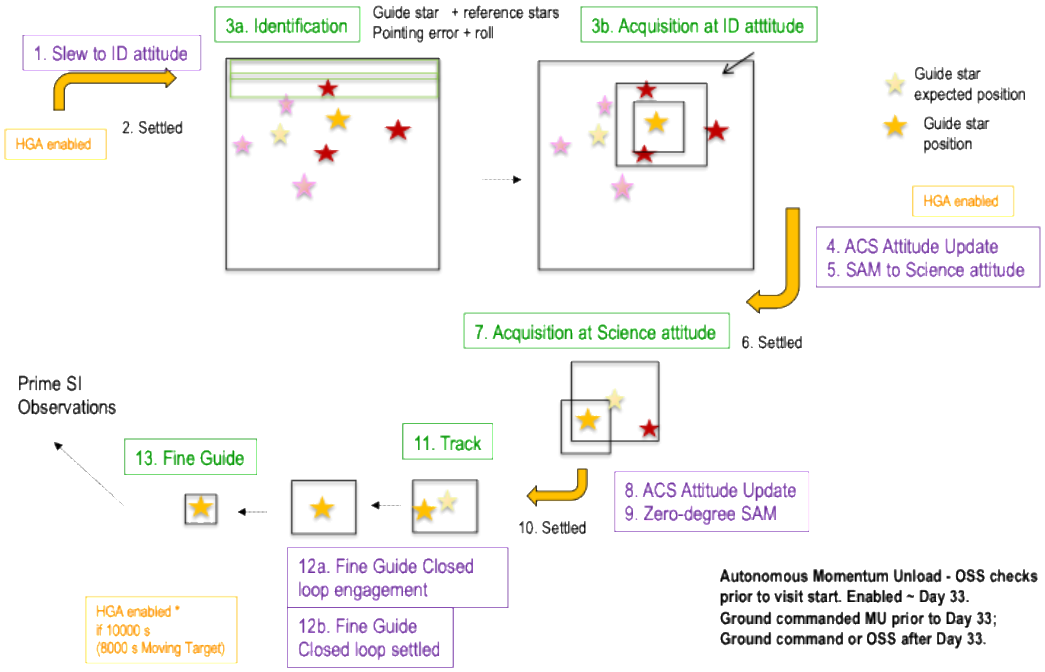


Figure 1. Pictorial flow of engaging closed loop guiding

Figure 2 shows how things actually look on the detector images to illustrate the operations to achieve closed loop guiding. (1) the Planning and Scheduling System places a given science target within a science instrument aperture, and at a selected spacecraft roll angle determines the patch of sky that falls upon the two FGS guide channels and queries the Guide Star Catalog for candidate GSs. A guide channel (G2 in this example), guide star, and Reference Stars (RSs) are selected and specified in the visit file. The visit file is populated with the desired location of GS and RSs on the selected detector along with its expected FGS measured countrate and countrate uncertainty (i.e., +/- range). (2) As the visit commences, OSS commands ACS to place the GS (X,Y) location of the selected guide channel at the RA, Dec of the GS, (hence where the GS is expected to be in the subsequent ID image) and when settled at that attitude, commands FGS to execute the ID function, extracting stars detected in a 2024x2048 pixel image of its field of view. The observed pattern of stars is compared to those specified in the visit file. The guide star is identified.

Yellow triangles (RSs) and yellow asterik (GS) in the ID image indicate expected location of the stars, offset from observed positions due to small coarse point errors (~2" in this example). (3) Upon command from OSS, FGS FSW executes ACQ1 (128x128, pixel, 8.8"x8.8" image centered at guide star's ID location, i.e., the yellow box in the ID image) & ACQ2 (32x32 pixel image centered stars' ACQ1 location), whereby the guide star's position is determined with increasing accuracy, and reported to ACS for attitude knowledge update. (4) OSS commands ACS to slew to the science attitude (which may be different than ID attitude) with pointing error removed. (5) The ACQ1 and ACQ2 are repeated at the science attitude updating the error after that science slew and this is followed by TRK and the final transition to FG. For most observations, if possible, the ID pointing is selected to be the same as the science pointing for efficiency, to avoid a slew to science and incur less pointing errors, but for some observations like Bright Crowded Fields (see Section 2.2) and Moving Targets (see Section 2.3) the ID pointing will place the GS towards the center of the Guider field of view to allow a better chance of acquiring the GS and RSs on these fields.

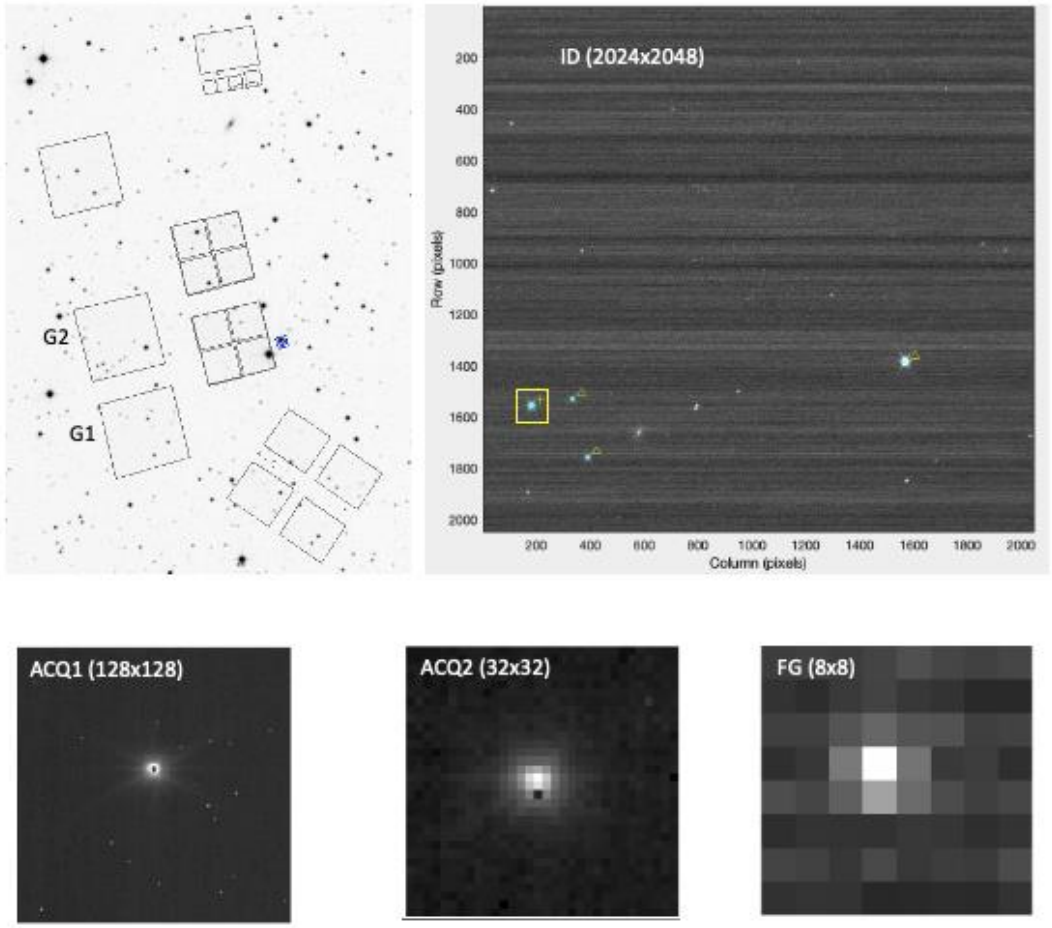


Figure 2. Top left is the GSC information for the GS and RS selections. Top right is the actual FGS G2 ID image as selected on the top left. Yellow box in ID image corresponds to size of ACQ1 subarray (8.8"x8.8"). The ACQ2 (and TRK) subarrays cover 2.2"x2.2" of sky, and FG subarray covers 0.51"x0.51".

For solar system object observations (i.e., Moving Targets) the FGS remains in TRK mode in closed loop operations with ACS, still providing a centroid every 64 ms with the exact location of the GS but being able to move the 32x32

pixel TRK window as the GS is drifting in the FGS Field of View (FOV) because the ACS is moving the Observatory commensurate with the science moving target, to keep the science target steady in the Science Instrument FOV. The visit file provides ACS with the GS ephemeris that specifies the track of the GS across the guider.

In ID Mode for non-Bright Crowded Fields (BCF), FGS reads out the entire detector (save for 12 rows at the top and bottom) in a series of 64-row strips overlapping 8 rows to account for Observatory drifting during the reads. A list of candidate Bright Objects that match the information given on the visit file for the GS and Reference stars is compiled from the image data by the FSW algorithm and used to attempt to identify that GS plus a variable number of Reference Stars. During Acquisition, the transition between ACQ1 to ACQ2 happens autonomously if ACQ1 is successful in finding the GS. In TRK mode FGS autonomously moves the detector window to keep the GS centered in the 32x32 pixel TRK box while providing the centroid information to ACS every 64 ms; once ACS declares the closed loop is settled, FGS will be commanded to transition to FG where an 8x8 pixel fixed window centered on the location of the GS is read at a cadence to generate a centroid for ACS every 64 ms. ACS is responsible for keeping the GS within the fixed FG window by adjusting the FSM based on the information from FGS. For all the guider modes a series of centroid quality indicators are generated (e.g., related to expected GS brightness, PSF height, width, delta signal, delta noise, etc.) and if any are not within acceptable thresholds that centroid will be marked as bad and not used by ACS in its FSM position calculations. For more details on the interactions between FGS and ACS, and pre-flight testing, see Vila et. al. [7].

The flow captured in Figure 1 is the baseline for operations on JWST as far as engaging closed loop guiding. However, Observatory efficiency paths were identified prior to Launch in coordination with ACS based on the expected accuracy of the various slews and their settling time. Thus for visits that slew to a location that is closer than 5 arcmin from the previous location up to 25 arcsec (such as mosaics), the initial ID and ACQ activities can be skipped and FGS can be commanded to enter directly at ACQ at the science attitude once the ACS slew to the new science location has settled. For visits where the Science Instrument needs an offset from 60 mas up to 25 arcsec from the current pointing OSS can command FGS to enter directly into TRK after ACS has completed the offset as the ACS pointing accuracy will be sufficient for the GS to be within the TRK box (2.2"x2.2") used by FGS to find the GS. For Science Instrument dithers of 60 mas or less FGS can remain in closed loop FG and the new dither location is achieved by ACS with FSM offsets. All these paths help to improve the JWST efficiency for observations. More details of the operations of JWST can be found in Hunter [8].

Each visit file uploaded on board can include up to 3 GS candidates (and associated Reference Stars) for either guide channel, if such stars are available. The first candidate GS is attempted up to three times in ID. If the GS is not found the 2nd GS, if available, will be attempted up to three times. If ID fails on the second GS, the third candidate GS, if available, is attempted. If ID is successful for a particular GS but ACQ is unsuccessful there are no re-tries in ACQ and the visit will move the ID to the next GS candidate. If ACQ is successful for a GS but TRK is unsuccessful, a second attempt from ACQ will be attempted. The possible reasons for not being able to achieve closed loop guiding are captured in Section 5.2.

*2.2 Bright Stars and Crowded Fields*

It was identified prior to launch that bright stars (J<14.5) would saturate in the ID and ACQ1 mode due to the longer integration readout times (~0.34 s) for those modes. Once getting to ACQ2 and TRK/FG the saturation would resolve itself due to shorter integration times (~50 ms) for smaller subwindow readouts (these modes set the GS bright limit at J = ~12.5). The visit commanding includes the uncertainty threshold for the commanded GS and RSs counts, i.e.,

the tolerance in the range of counts that the GS and each RS can have to match the expected brightness from the catalogue. For bright stars that would saturate in ID and ACQ1 this threshold was increased through the Guide Star Selection System (GSSS) so it would cover the range needed for all the guider modes. For example, a very bright guide star with a Fine Guide countrate (CR) of 1,300,000 counts/sec could have an ID CR observed to be only 450,000, so the visit file needs to specify a +/- threshold larger than 850,000 for a successful ID outcome. Figure 3 captures a pictorial summary of how the GS counts would appear as it moves through the guider modes and how the threshold needs to be increased to capture all of them. In the Figure, 'ID in' is the expected GS counts based on the Catalogue. The blue vertical lines are the uncertainty on those counts. The uncertainty needs to be large enough to capture 'ID out' and 'ACQ1' counts that will be lower due to saturation. As seen in the Figure, ACQ2, TRK and FG give the expected counts for the visit.

Taking into account the throughput of the FGS in JWST it was determined that the GSC larger uncertainty threshold needs to be triggered for bright saturating stars whose 3x3 pixel count rates ≥ 511,116 counts/s, and in those cases the threshold is increased by a factor related to the brightness of the stars by setting it to (countrate – 332226), which satisfies the image scanning algorithm that searchs for saturated pixels of the bright stars.

For stars below those counts at the start of the JWST on orbit operations the GSC threshold was 30%. During commissioning it was determined that this threshold could be increased to 35% and two years after operations, in December of 2024 it was increased to 40%. The main contributing factors to increasing this threshold is to capture GSC uncertainties on the classification of GSs – i.e., sometimes the selected GS turns out to be a galaxy or a double star and the counts seen by FGS are lower than those commanded in the visit and increasing the allowed uncertainty would help to allow some of those visits to be successful in spite of the misclassification – and the point source Photo Response Non-Uniformity (PRNU) seen on the FGS detectors (particularly on G1) during operations where the counts seen for a Guide Star can sometimes vary up to 30% when dithering to certain pixels – more details captured in [13].

The early mission commanding on orbit applied the same threshold throughout all the guider modes – i.e., each guider mode has to identify the correct GS whose reported counts must match the counts within the uncertainty threshold indicated on the visit file. A further improvement implemented during normal operations was an update on the OSS to change the threshold from the one commanded on the visit to the default for non-bright stars (originally 35%, now 40%) after proceeding to ACQ2 and TRK and FG. In those modes the counts for the stars, even for bright ones, would not be saturated and would match closer those from the catalogue. This helped to avoid some cases where an incorrect fainter GS was identified in ID and ACQ1 and still proceeded through ACQ2 and TRK/FG though it was by then clear that the counts reported were too far off from the commanded ones but still within the larger threshold used for bright stars.

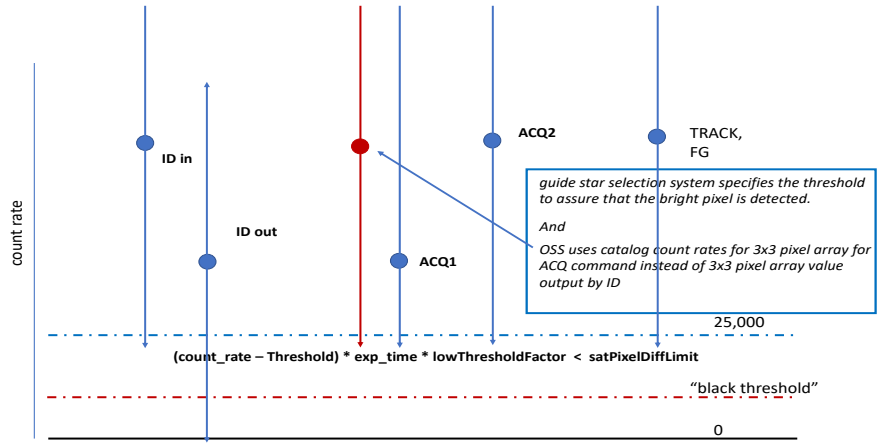


Figure 3: Pictorial representation of the counts seen for bright stars through the guider modes due to saturation in ID and ACQ1

Another path identified prior to launch was related to Bright Crowded Fields (BCF), which are pointings in the sky where many bright stars would be present in the guiders FOV. This could cause too many candidates to be identified as possible GSs during the ID scanning because for some star fields, up to 300 stars would saturate and appear with a similar 3x3 pixel countsum that would match those on the visit file within the larger brightness uncertainty thresholds needed for those fields. The ID algorithm can store up to 100 candidate objects to be the GS and if the whole guider FOV is read it is likely that the intended GS won't make it into that list. Accommodations were placed for the Guide Star Selection System to identify a field as a BCF and with that flag in place, OSS commands FGS to read a smaller portion of the FGS FOV (12 strips instead of the default of 36 for non BCFs) and also updates some of the parameters in the ID algorithm that can be tuned as a table load for those types of fields. An image of a crowded field is shown in Figure 4.

Further improvements were identified during normal operations for observations towards the center of the Galaxy, Sgr A* area. These were an improvement on the GSC from the one used during commissioning and earlier normal operations by adding the Galactic Nucleus Catalogue (GNC), Nogueras-Lara et al. [9], as well as the Gaia ER3. Figure 5 shows a Sgr A* field and the improvements in the Catalogue. Analysis also showed that the algorithm converting the GNC photometric information to Near Infrared counts underpredicted what FGS would see by a factor of 1.25 to 1.9 due to the extreme reddening in this area of the sky. An average scale factor of 1.5 was put in place to apply to the GS counts for visits on this area of the sky. These improvements gave a success rate looking towards the center of the galaxy of ~ 75% in terms of identifying the correct GS. Further analysis of the flight data identified a possible FGS algorithm update, in the process of being implemented with a FSW patch, to better calculate the counts in ID and ACQ1 for the saturated stars in bright fields. With this improvement in place it is expected the successful achievement of closed loop towards the center of the galaxy to move to ~ 90% success rate. As shown in more detail in Section 5.2 the success rate overall for the FGS in JWST is ~ 96% in finding the correct GS and allowing all science observations to proceed.

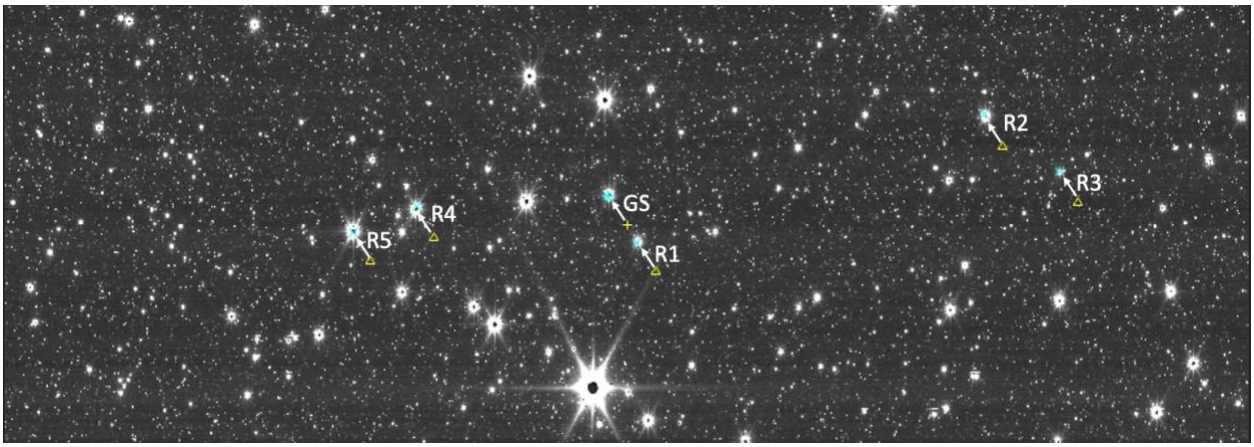


Figure 4 – Example of the FGS ID Bright Crowded Field image in a Sgr A* pointing. The triangles show the expected locations of the GS and 5 RSs used for this visit and the arrows show where they were found after the slew pointing error to the ID location.

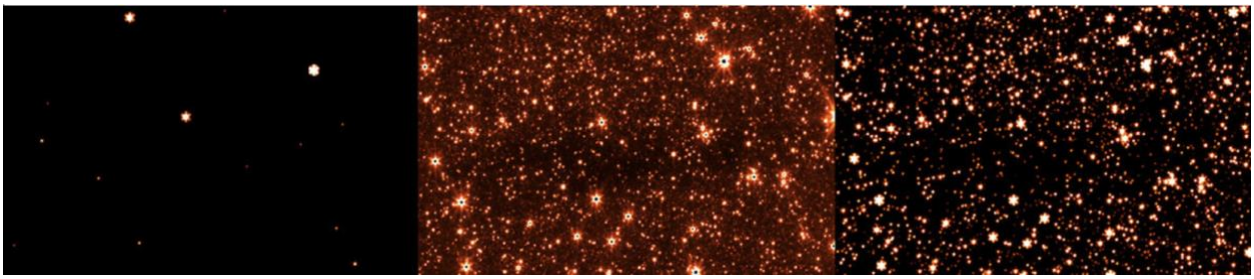

Figure 5 – Simulated and observed FGS images of a Guide Star field for a Sgr A* science program. Left: Simulation based upon the contents of GSC2.4.3.1 which was the operational Guide Star Catalogue at the time of these observations and what was used as input for the GS/Reference Stars on the visit file. Center: Image captured by the FGS of the same area of the sky, as part of the Guide Star acquisition process in ID, showing saturated cores of bright stars. Right: Simulation based upon the contents of the GNC, now part of GSC3.0, demonstrating the remarkable correlation with the near infrared sky observed by FGS in the neighborhood of Sgr A*. These images cover a 48"x33" patch of sky, which is about 8% of the FGS detector.

*2.3 Moving Target Operations*

JWST can observe objects within the solar system from Mars outward. To do these types of observations the FGS uses its Moving Target (MT) mode, where the detector keeps being read in TRK mode still in closed loop with ACS, and the location of the TRK 32x32 pixel window moves as the GS moves in the FOV. The trajectory (the opposite of the solar system target's ephemeris) needed for the GS is uploaded on board as part of this type of observation to allow the solar system object being observed to remain stationary in the SI FOV. The initial portion of the acquisition of the GS for ID and ACQ at the ID attitude, as well as ACQ at science and the entry into TRK are the same as for a normal non-Moving Target observation. Once the Guide Star is found it is kept in the TRK box until the start time needed for the science observation when the science target is at the required location in the Science Instrument field of view– at that time the TRK GS motion will start.

Figure 6 shows a pictorial summary of the Moving Target concept of operations. The original requirement was for FGS to be able to track objects moving up to 30 mas/s. During commissioning it was validated that the tracking rate could extend to ~ 70 mas/s. With some updates on the track window, update rate and other parameters, in the successful observation of the Double Asteroid Redirection Test (DART) mission, a rate of ~ 110 mas/s was achieved, significantly exceeding the originally designed tracking speed. With this successful demonstration currently JWST supports observations of targets moving up to 75 mas/s with the possibility of observations up to 100 mas/s being considered for special situations.

When the GS moves more than a certain amount from the center of the TRK box, FGS FSW sends a command for the detector to re-center the GS in a new TRK box and marks centroids as bad until it hears back from the hardware telemetry that the data is coming from the new detector location. It had been analyzed that ACS could tolerate up to 5 bad centroids in a row without affecting performance. The flight data shows that FGS always marks ≤ 3 bad centroids during these track window updates. To improve performance for MT observations the change in Guide Star location required to trigger a TRK window update was relaxed from 2 pixels to 4. ACS does not use FGS centroids marked bad so this relaxation on the TRK box trigger to move provided a better performance for faster solar system targets without impacting slower ones.

The Noise Equivalent Angle (NEA) requirement for MTs was 6 mas for a GS above a certain brightness. FGS is exceeding this requirement with typical MT NEAs ≤ 3 mas (see section 5.1 for more discussion on NEA).

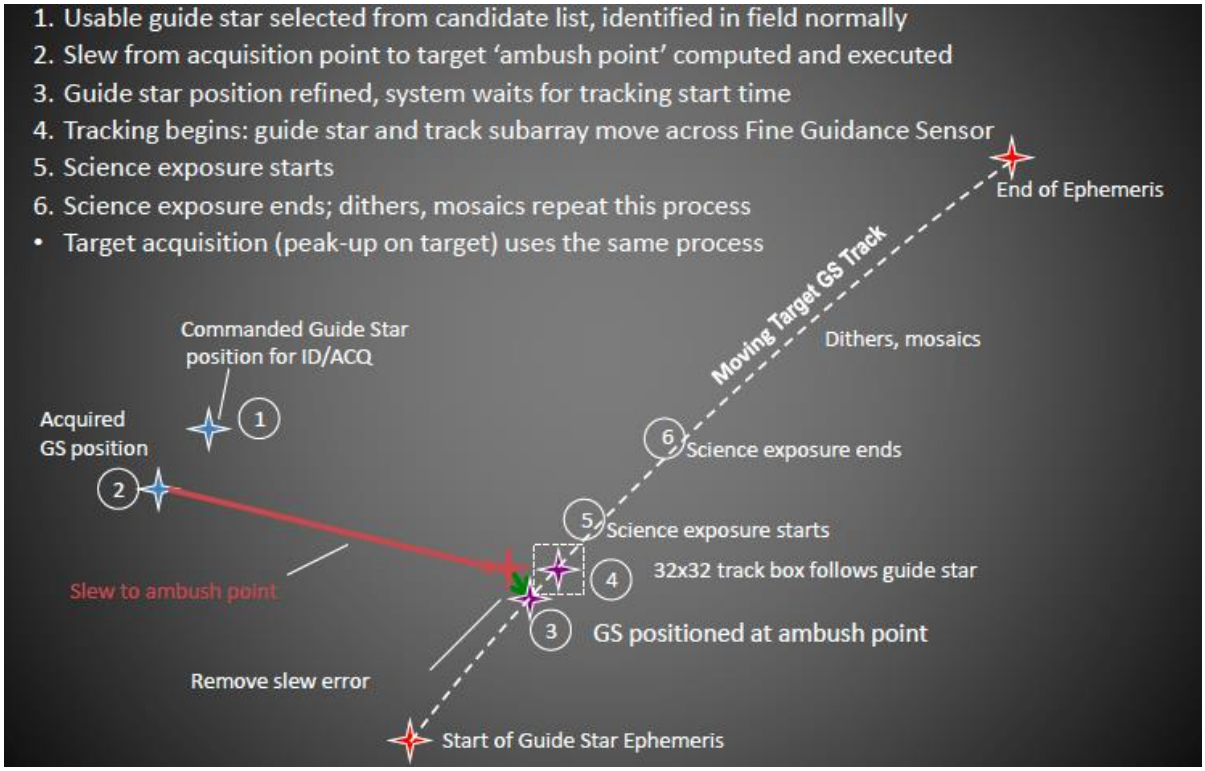


Figure 6 – Pictorial representation of Moving Target operations

### *2.4 Timing*

FGS had various guiding timing requirements in order to handshake with ACS through the different guider modes. All of the requirements are being met in operations:

- The timing to complete ID is less than 130 s, typically ~ 115 s – this timing depends on the number of Reference Stars and the number of candidate GSs found for a particular field. In the case of BCFs where the bright object list of 100 candidates is filled the ID timing is actually ~ 50 s because a smaller portion of the FGS FOV is read (12 strips instead of 36 for non-BCF IDs). To improve performance the FGS detector is set for the ID readout in parallel with the slew to ID, though the exposures do not start until ACS declares the slew as settled.
- The timing to complete ACQ meets the 15 s requirement. The timing is closer to ~ 11 s for the ACQ at science as the FGS detector is set up in parallel with that slew to science though again the exposures do not start before the slew is declared settled by ACS.
- For TRK and FG the centroids need to be generated every 64 ms – there is a healthy margin in the worst case for TRK of ~ 10 ms and in the worst case for FG of ~ 3.5 ms between when the centroid is ready and when ACS picks it up at the 64 ms cadence.

## 3. Guiding in Early Commissioning during Mirror Alignment Activities

### *3.1 FGS Commissioning Activities*

After the launch of JWST, the commissioning of the entire Observatory from the Spacecraft, Telescope and Scientific Instruments followed a well-planned sequence. The overall commissioning timeline as originally planned is shown in Figure 7. Figure 8 shows the major commissioning milestones for FGS. The FGS came into action very early when the Optical Telescope Element (OTE, basically the mirrors and surrounding structure) was commissioned, because fine guidance control was necessary to support the image-based phase retrieval methods, which operated under Wave Front Sensing and Control (WFSC). This is discussed further in Section 3.2. JWST launch occurred on Dec. 25th, 2021 at 12:20 UTC. Thus, elapsed time from launch (L+) can be found by adding 5.514 days to the 2022 day of year (DOY) at 00:00 UTC.

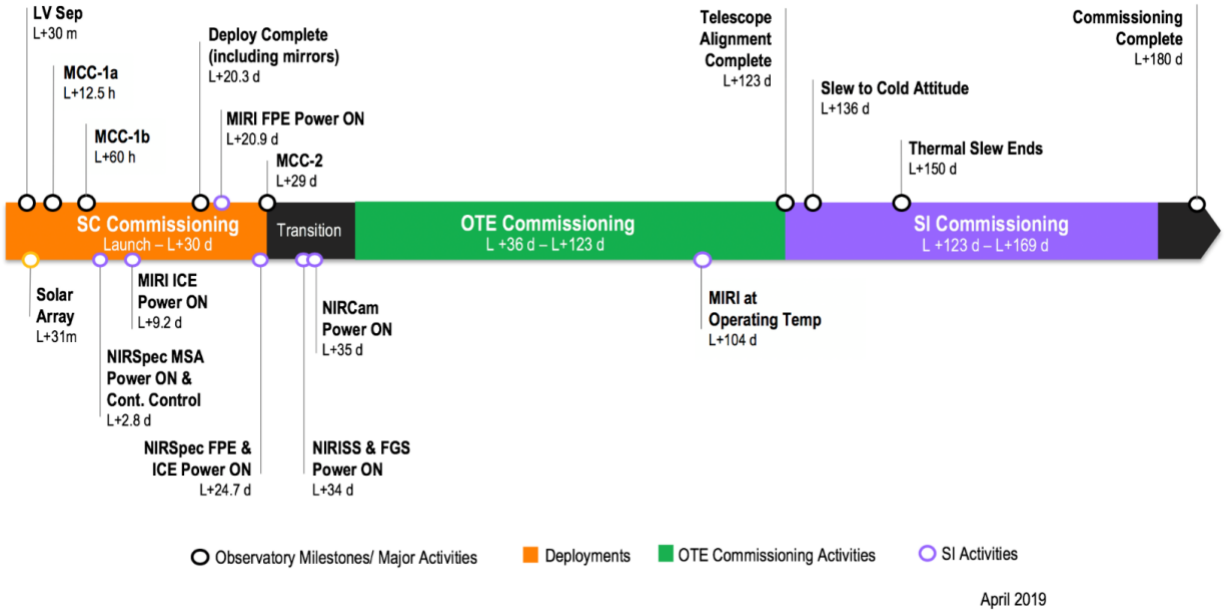


Figure 7: JWST Commissioning Timeline Overview (as planned)

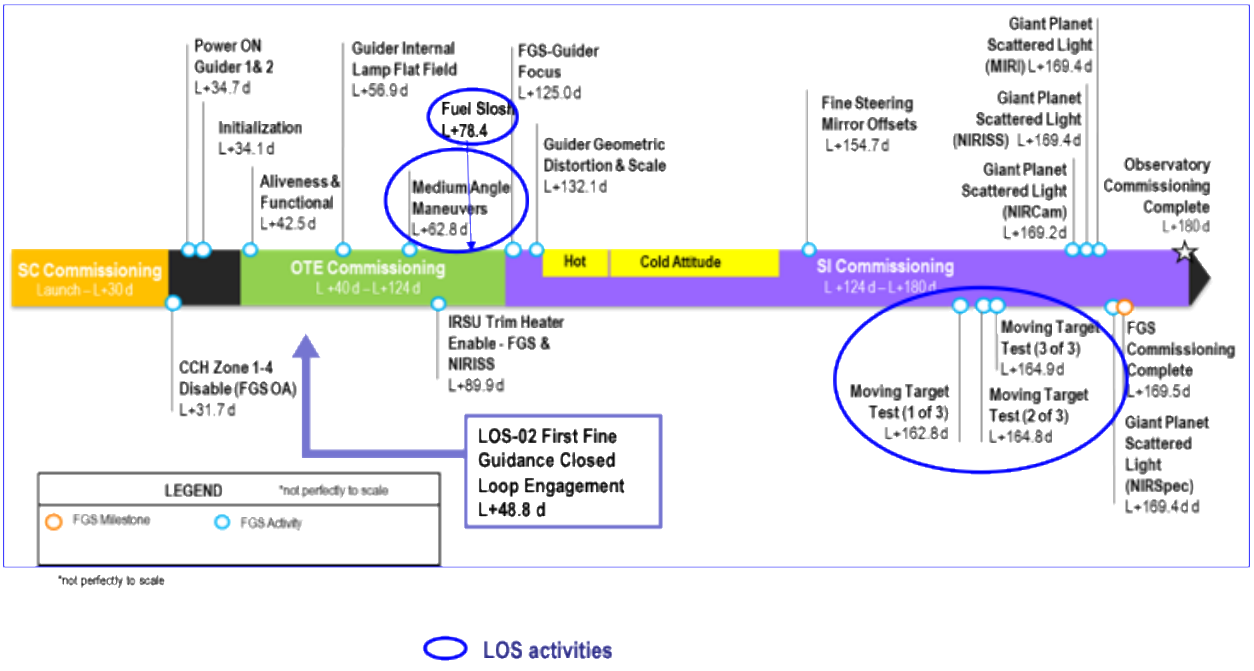


Figure 8: FGS Commissioning Timeline Overview including activities defined as LOS (Line of Sight) (as planned)

After FGS power on and initialization that occurred on day L+34, periodic FGS images were taken starting when the detector temperatures reached ~ 80K. This allowed monitoring of the bad pixel map population on the detectors as

a gate for the start of guiding operations. It was noted that in particular the bad pixel population for Guider 1 was much higher (~60%) on orbit, in particular around the edges of the detectors at those warmer temperatures than had been the case during ground cryo tests which was not an expected result – see Figure 9 for a comparison of the G1 image corner at 80K on orbit vs the one taken during the last ground cryo campaign. This was initially a source of some concern. However, FGS images continued to be taken periodically as the detectors cooled down and it was eventually observed that those excess hot pixels did continue to settle as the temperatures went down. The first guided activity was called LOS-02 when the FGS detectors were ~65K, prior to the 40K cold plateau for which the bad pixel map was designed, so there were still excess hot pixels that were not included on the bad pixel maps on board. A process for regular updates on those maps was developed and details are included in Section 4.1.

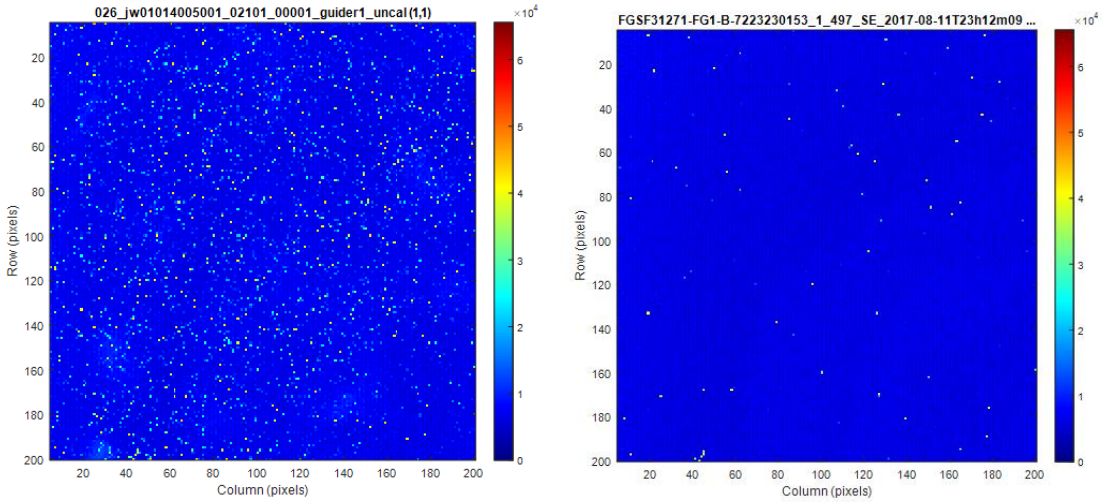


Figure 9: Guider 1 Top Left Corner Showing Border hot pixels at ~80 K (left) vs. ground cryo test (right)

It took approximately two months from the time the FGS was powered on until the detectors were at their nominal operational temperatures ~40K and when the mirrors were fully aligned. A detailed description of the FGS activities for operations is beyond the scope of this paper but a summary of some of them is captured as follows:

- FGS had to be slightly defocused to optimize guiding operations. Its Fine Focus Mechanism (FFM), common to both guiders, was adjusted from +3.2 mmOTE to +2.2 mmOTE, which actually represented a slight *defocus*, since measured star PSFs at the launch best focus location were determined to be slightly too sharp. For centroiding purposes, it is preferable for Guide Star energy to be slightly defocused onto adjacent pixels. This defocusing was chosen in the direction closer to the center of the Fine Focus Mechanism (FFM) motion range. The analysis tools and process for identifying best focus were developed and exercised during the ground cryo campaigns. A best common focus was chosen based on the data from both guiders in different field points on their FOV.
- Calibration of the geometric distortion across the FGS FOV was carried out by observing the JWST's calibration field in the Large Magellanic Cloud (LMC). The LMC calibration field is a star catalog that was constructed from observations obtained by the Hubble Space Telescope at two epochs and from the Gaia DR2 catalog - see Anderson et al. [10]. Distortion coefficients identify the delta between an ideal detector to the real detectors and are used on board by the FGS FSW and also on the OSS FSW to convert between Ideal Pixel coordinates to Real Pixel coordinates. Calibration was performed using methods similar to those

as described in Sohn et al. [11], and the resulting distortion solution has uncertainties at the level of ~3.5 mas rms per axis. A checkout of these coefficients is performed periodically, about once a year during normal operations. No other updates since the one done during commissioning have been identified to date.

### *3.2 FGS Operations during JWST Mirror Alignment Activities*

During early commissioning while the JWST mirrors were being aligned multiple activities were needed to ensure successful closed loop operations to allow the mirror alignment activities to proceed. Figure 10 provides a more detailed OTE commissioning timeline segment during which OTE alignment occurred showing many of these activities. More details on the OTE activities and performance can be found in McElwain et al. [12].

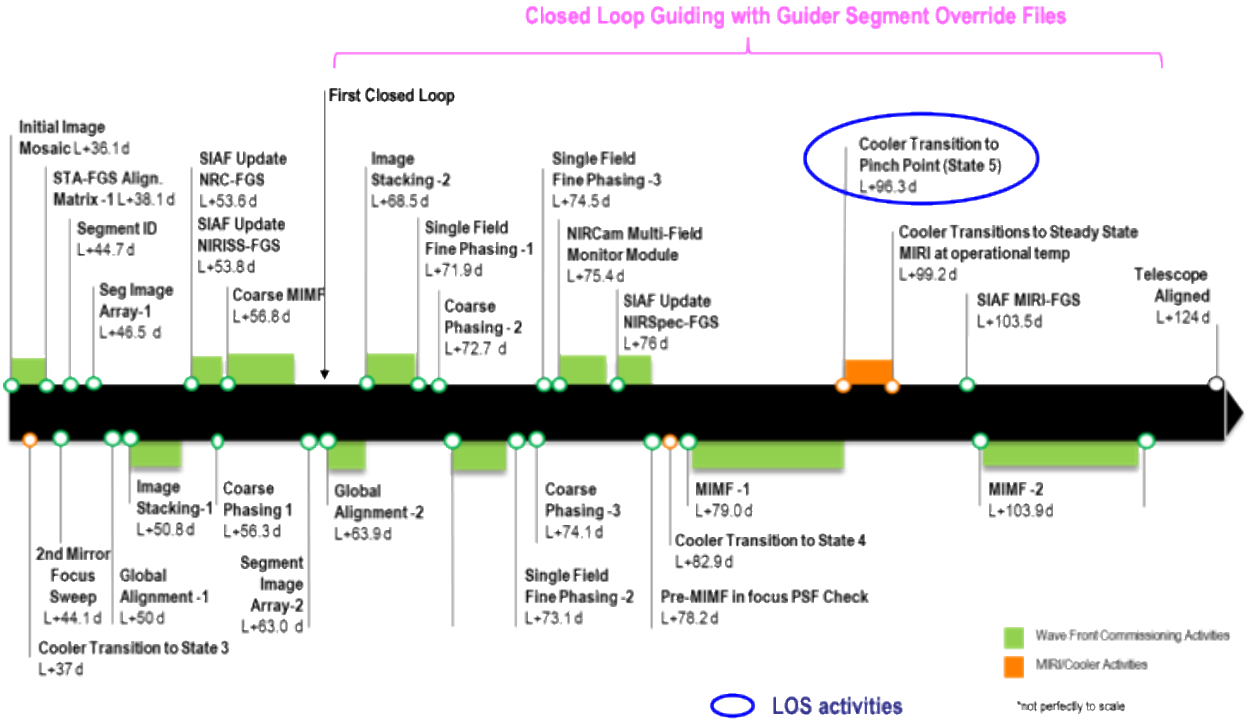


Figure 10: Detail of the OTE alignment phases where FGS had to guide using override files (SOFs or POFs) as described in this section

During the first phases of aligning the 18 primary mirror segments, every star appeared as 18 separate stars in the FOV, one on each mirror segment. As these segments were not yet in phase nor in focus, their PSFs were highly distorted. The GSSS chose suitable GSs and Reference Stars for the OTE activities, but this information needed to be overwritten to match the segment mirror positions and the 18 stars that would be seen. The PSFs of each of those 18 stars were different depending on the state of alignment and focus for that particular segment. This meant that for each visit the information from the catalogue had to be overwritten replacing the GS location and counts with

the expected location and counts for the PSF on the segment to be used for guiding. Similarly the Reference Stars information had to be replaced. Various analysis tools were developed by the Wavefront Guiding team supporting the OTE and the FGS team supporting on the FGS console to predict the expected PSF counts and locations of the various mirror segments and validate that closed loop guiding would be successful before sending the information to the Planning & Scheduling team to overwrite the visit files. During the mirror alignment the mirror segments would also be moved so this information was also needed to be able to select suitable segments that would remain stationary for the guider. The Wavefront Guiding team worked with the FGS team to validate and provide Segment Override Files (SOFs), that change counts and locations, or later on in the mirror alignment process Photometric Override Files (POFs), that change the counts only, with the information for each mirror segment to correctly use Guide Stars and Reference Stars.

Figure 11 shows on the left panel a NIRCam image of a bright star observed in coarse pointing during the alignment of the segments (a drawing of a star was placed at the center of the image to illustrate the commanded position of the star). All segments that were then identified had been placed in a hexagon shape. Such an image was analyzed by the FGS team in order to select the segments most favorable for FGS operations. The right top panel shows an FGS TRK image of the segment that was selected as the guide segment for the first successful closed loop guiding (LOS-02) and in the lower right is a plot of all the centroids reported every 64 ms, showing the spread of the Noise Equivalent Angle (NEA) on this first closed loop guiding (more on NEA in section 5.1) showing ~ 11 mas, meeting the needed requirement of 20 mas on this phase of the OTE alignment process.

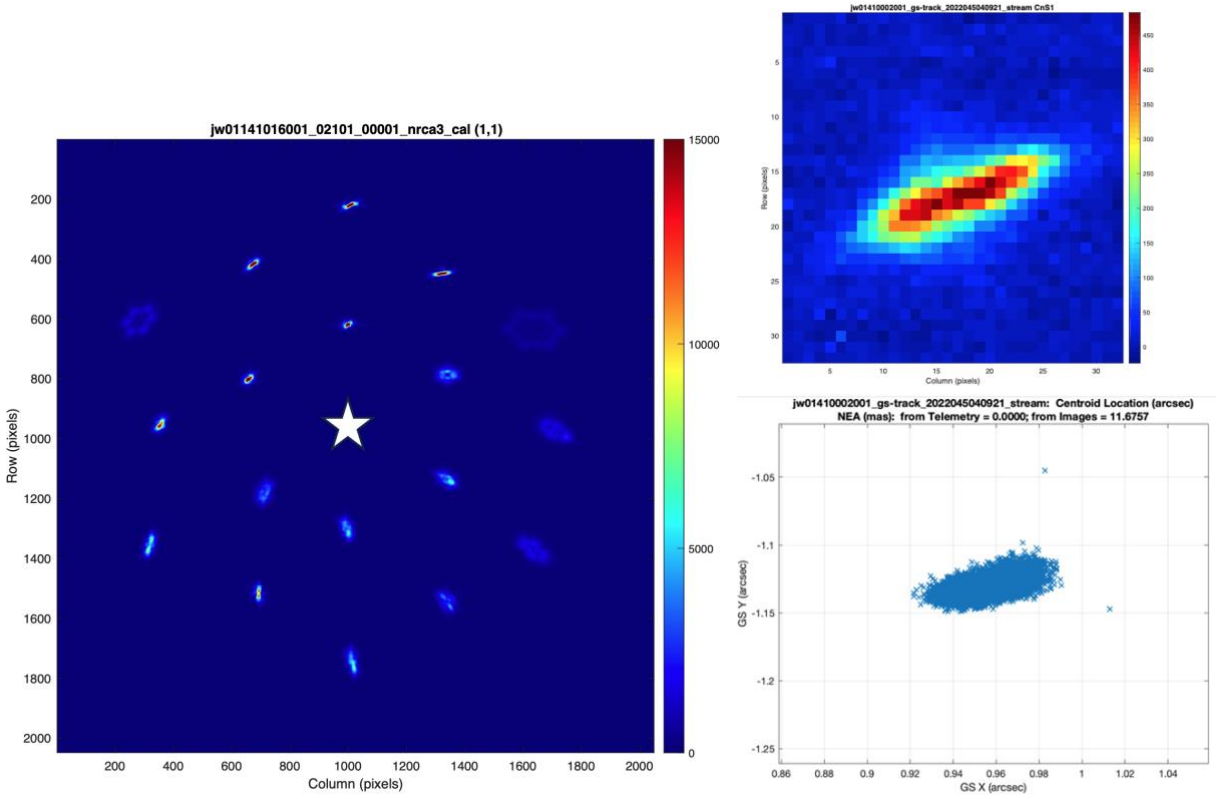


Figure 11. On the left a NIRCam detector image of a bright star observed during OTE alignment (drawing of star at center of image illustrates commanded position of a bright star on the detector). On the right the Track Image of

the PSF that achieved successful closed loop. Lower Right: the centroids reported, indicating a larger NEA expected at this phase of mirror alignment.

Prior to launch optical models were used to predict possible PSF shapes which might occur during the OTE activities. These had been generated in collaboration with the OTE team and injected into the FGS simulators in order to test and validate what actions would be necessary during commissioning to ensure that the engagement of the closed loop would be successful. These many rehearsals were invaluable to ensure the successful operations on orbit during this phase of commissioning. This was also practiced multiple times on the telescope simulator in various FGS and wavefront rehearsals prior to launch.

Another challenge faced by the FGS was the activity related to multi-field alignment. As the alignment of the telescope was done to the NIRCam instrument field only, it was important to make multi-field measurements and assess the alignment of the telescope across all Science Instruments and FGS. These measurements were made at several predetermined positions for each instrument (Multi-Field, Multiple Instruments: MIMF). At each of these positions, images from each instrument were taken at different focus positions always under fine guidance control. Figure 12 compares the range of GS PSFs that the FGS had to accommodate for these observations. The left panel shows a nominal GS PSF while in TRK when the telescope is at its nominal focus position. The right panel shows the same GS in TRK, but with the secondary mirror defocused by +100 μm.

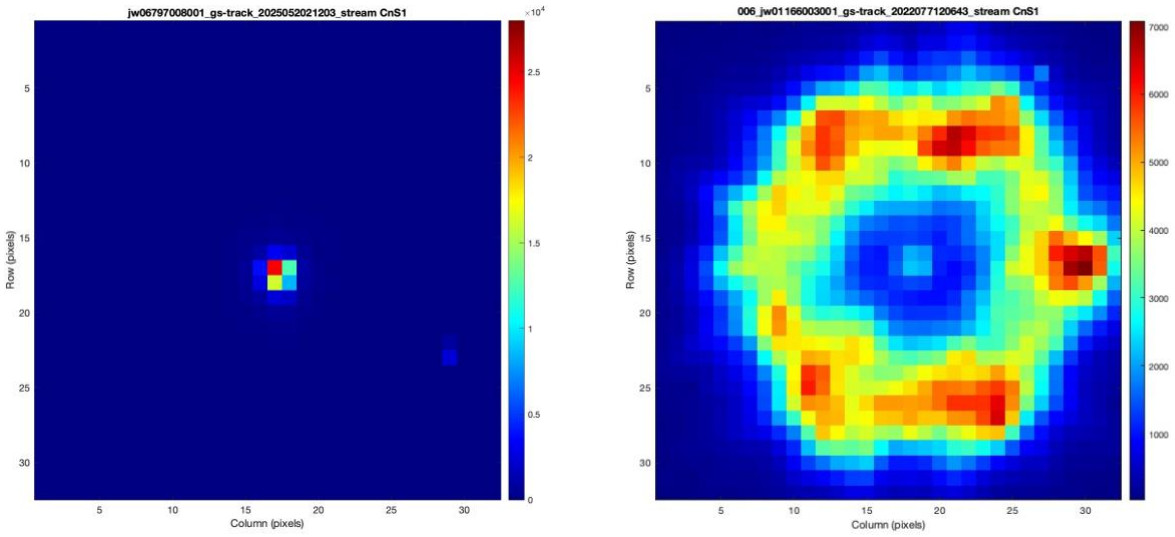


Figure 12. Right panel: Nominal GS PSF in TRK. Left panel: GS PSF in TRK when secondary mirror is defocused by +100 μm.

The other accommodation needed on FGS during the early commissioning activities to be successful with all the GS PSF changes mentioned was to update some of the FSW parameters used for ACQ2 and TRK to be able to declare the aberrated/defocused PSFs during that period as good to pass the quality indicator threshold check used by FGS, so the closed loop with ACS could be settled. During most of the mirror alignment activities FGS remained in closed loop TRK mode (32x32 pixels window) as the PSFs were too large to fit properly in the smaller FG window (8x8 pixels) used for normal operations. The mirror alignment activities ran in two main phases to improve the overall alignment. FGS transitioned to FG for the end of the first phase and back to TRK for the start of the second phase, and returned

to the default FG at the end of the second phase when the OTE team declared the JWST mirrors met all the alignment requirements. The parameters updated were related to relaxing the expected PSF width and height, the window size used by the software to calculate the centroid and the definition of what would trigger a bad delta signal and delta noise for the centroids' calculations. The FGS team carried out many Telescope simulator tests prior to commissioning with many examples of possible early commissioning PSFs provided by the OTE team to confirm closed loop operations during this critical period of commissioning and confirm the FGS FSW parameters to be updated.

While many of the challenges associated with attempting the first closed loop activity were understood and planned for prior to launch, one unanticipated challenge which manifested in real time was related to a residual drift in the Observatory pointing after performing the slew to bring the targeted Guide Star segments onto the FGS detectors. After performing this slew, there was typically a variable duration during which the Observatory pointing continued to drift, before settling to a static pointing. This could result in the locations of the segment PSFs changing during Identification attempts, and therefore making it impossible to match Bright Objects between the 2 separate reads in the Identification process. Eventually the first closed loop was successful and follow on guided activities for the mirror alignment continued with different closed loop guiding challenges through the following two months until the mirror alignment activities were complete.

## 4. Summary of Improvements Since Launch

### *4.1 Bad Pixel Map Updates*

Data tables containing the locations of known bad pixels were generated and maintained throughout the ground cryogenic testing period. This process resulted in the initial "Rev 64" version of guider Bad Pixel Maps (BPMs) which were loaded prior to launch and designed for FGS operation at 40K. In the initial revision of the BPMs, there were a total of 11919 bad pixels of various types identified on the Guider 1 detector (representing 0.285% of the active pixel area) and 21508 bad pixels identified on the Guider 2 detector (representing 0.515% of the active pixels). This is shown in Figure 13.

The final 40K ground images used as inputs to the bad pixel maps were taken during the cryo test campaign in 2017, while JWST was launched at the end of 2021. The bad pixel population had been previously observed to change slightly with thermal cycling and with accumulated radiation damage, so it was anticipated that an on-orbit update would be necessary as part of the Commissioning phase in order to ensure optimal Guider performance.

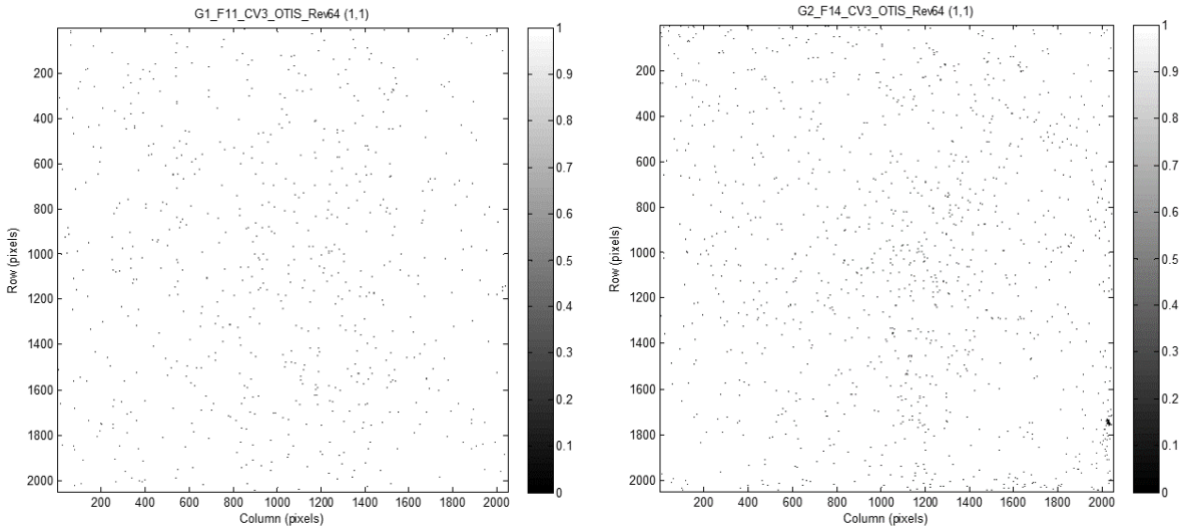


Figure 13: FGS Bad Pixel Maps at Launch (Rev 64). Left: Guider 1 initially had 11,919 bad pixels (0.285%). Right: Guider 2 initially had 21,508 bad pixels (0.515%).

The first bad pixel map update for operation was completed on May 2, 2022. Soon after the end of commissioning a monthly cadence to upload new bad pixel maps on board was established – with typically ~ 30-50 new hot pixels found per guider each month due to ongoing radiation impacts damaging individual pixels.

During on-orbit operations, modifications to some of the bad pixel classification and counting schemes in order to optimize on-orbit guiding performance resulted in a re-baselining of the original bad pixel maps from the initial "Rev 64". This resulted in some "resets" to the total number of bad pixels stored during the course of normal operations as described in [13]. At the time of writing this paper with "Rev 95", the Guider 1 BPM contained 11503 bad pixels (0.287%), and the Guider 2 BPM contained 13727 (0.343%). Now that the classification and counting methodology for on orbit operations has been stabilized, it is anticipated that the populations will continue to demonstrate the steady growth rate observed to date of ~ 40 pixels per month, due to approximately steady radiation flux at the JWST orbit. Figure 14 shows the incremental growth in Guider 1 and Guider 2 bad pixel populations in the second and third years of normal operations.

Note that if the bad pixel populations continue to grow by ~40 pixels per month, per detector, then over 10 years the total populations would only grow by 4800 pixels per detector. At this rate, the bad pixel populations would remain under 0.5% of the total active pixel area, and would not result in any significant impact to Guider performance. It is not known if any detector aging effects might eventually cause the rate to increase over time.

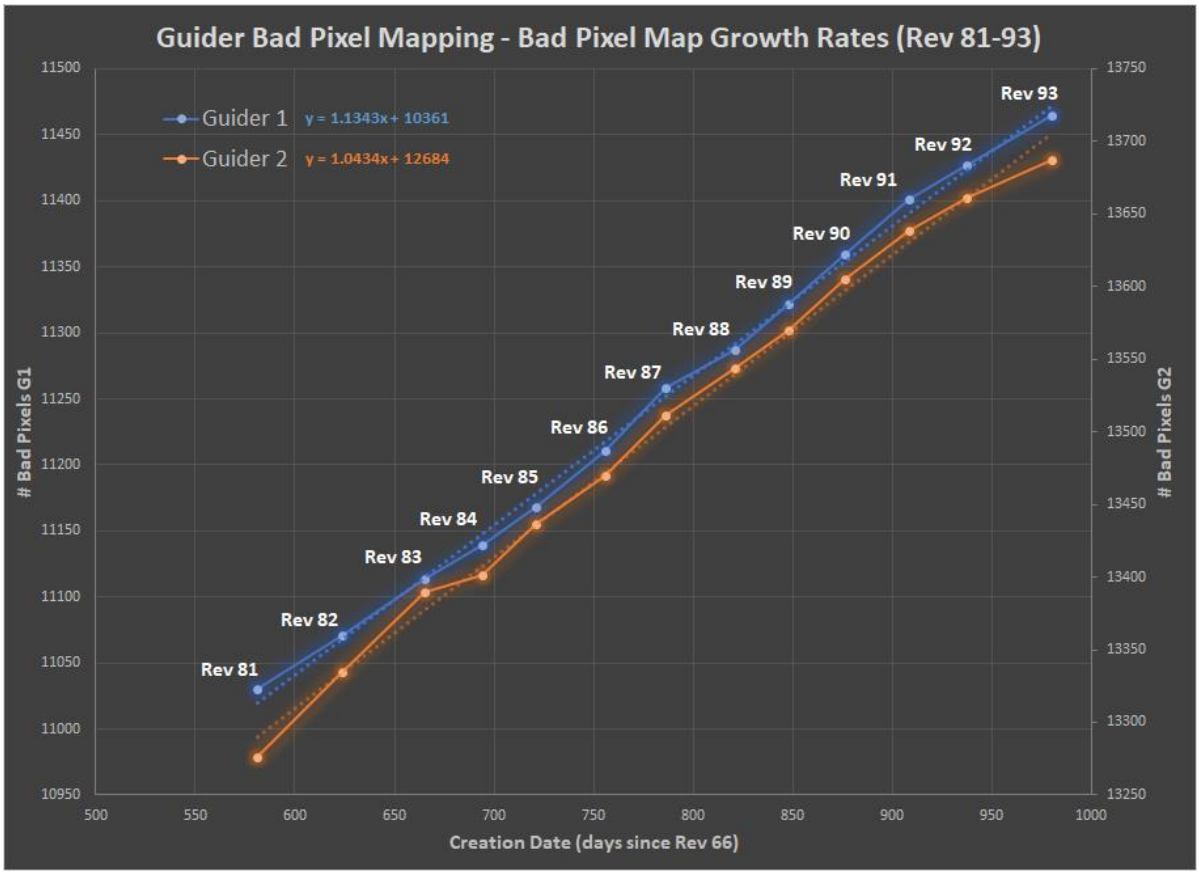


Figure 14: FGS Bad Pixel Map Growth Rate during Normal Operations

### *4.2 FGS FSW Configuration Parameters*

Some of the parameters optimized on the FGS FSW for operations include:

- Updating the parameter that identifies when a pixel is saturated. This parameter is the ADU counts that the FSW will use to determine that a pixel is saturated. That number covers a range as it is slightly different for all pixels, however one overall number needs to be used. The number was moved closer to the lower value of the saturated pixel distribution that had been chosen prior to launch (RawSatPixelLimit for G1 from 57000 to 54500 ADU counts and for G2 from 56000 to 53000 ADU counts). Note that there was not any characteristic shift in the values of the saturated pixels but in several instances it was observed that some saturated pixels were not being replaced in ID, resulting in poor estimates of the GS amplitude.

- Updates on some of the ID parameters used by the FGS FSW on the algorithm to find the correct GS to improve performance. During ID the detectors are read to generate two initial Bright Object Lists that are then blended into a single one including only candidate stars that appear in both. After this the ID algorithm runs a triad matching activity to isolate the best candidates for the GS and reference stars. The detailed information on the parameters used in this process is beyond the scope of this paper but they include: a

decrease of the parameter that controls the amplitude matching of candidate bright objects between the two bright object lists generated in ID (MergeIntensityPct parameter decreased from 0.8 to 0.7) to better bracket the observed performance range due to the higher than expected countrate variation with residual drift and pixellation (especially on G1); reduction of the parameter used to tighten the triad shape matching (Epsilon from 130,000 to 72,000); reduction of the allowed triad rotation angle error as ACS roll accuracy was found to be very good during normal operations (AttitudeError from 14.5 to 2 degrees); reduction of the allowed position error (AbsMatchError from 562.5 pixels to 220 pixels) – this is still larger than the OSS 10" check and allows FGS to find the correct GS in many cases even if the pointing error is larger.

- Update to ACQ1 parameters: to allow the GS to be further from the center of the ACQ box to tolerate larger pointing errors on ACS if the GS is still within the 128x128 pixels of the ACQ1 box (AbsMatchError from 54.8 to 60.0 pixels); a decrease of the parameter that controls the amplitude matching of candidate bright objects to match what was done in ID (MergeIntensityPct parameter decreased from 0.8 to 0.7).

- Disable delta signal/delta noise parameters. This is the variation in signal and noise in different reads that could indicate a possible erroneous GS, however on flight it was found these quality indicators are not needed.

- Update to the criteria that defines when the TRK box should be moved to keep the GS centered to allow better performance for Moving Targets at faster rates than the original MT requirement (SUBIWNUPDATECRITERIA from 2 pixels to 4 pixels) as discussed in Section 2.3.

- Fixed a couple of bugs on the FSW for Track impacting mostly Moving Target activities. The FGS FSW needs to access the bad pixel correction data for operations but should clear this data (and other variables) when exiting Track mode and was not doing so; there was an FGS FSW logic issue on the marking of bad centroids when the counter for the number of integrations rolled over.

Additional information and description of the updates listed above can be found in [13].

### *4.3 Guide Star Catalogue (GSC) and Guide Star Selection System (GSSS)*

Improvements on the Guide Star Selection System included: Adjustment to GSSS Guider 2 gain to increase Guider 2 commanded counts in visits [13]; Guide Star counts thresholds raised to 35% for commissioning from initial 30% and adjusted again in December 2024 to 40% for operations; Reference Star magnitude range (J= 10.0-18.0) and Guide Star range (J= 12.5-18.0); Moving Target Guide Star lower magnitudes increased to J=16.5 (G1) and J=17.0 (G2) which gives ~ 55,000 ADU counts/s on the FGS 3x3 pixel window as the lower range; ID pointing exclusion zone to not choose a GS closer than 15" from the edge of the FGS detector; Galaxies not to be used as Reference Stars (issues remain where GSC is not aware that a given celestial object is actually a galaxy and not a star; these are being corrected when discovered and those objects flagged as non-usable.

The GSSS also implements an exclusion zone of no other stars within 2 magnitudes of the GS within 6" to avoid spoilers within the ACQ box.

Other GSSS updates during normal operations include the prioritization of bright stars as candidates for GSs and the attempt to identify if there are bright objects (e.g. galaxy arms, globular clusters or other) in the FGS FOV near the selected GS.

JWST operations started with GSC 2.4.2. During commissioning the use of 2MASS magnitudes instead of Vista when available was included as well as the removal of duplicate entries due to the merging of catalogues (GSC 2.4.2.1). Further improvements were added during normal operations to move to GSC 2.4.3. A significant new release mentioned previously was GSC 3.0 (operational on 02/02/24 and used on orbit for the first time on 03/04/24) – this GSC is Gaia based for astrometric positions, proper motions, and parallaxes of all sources that map to Gaia objects, thus most JWST visits use guide stars that have 1 milli-arcsecond or better known absolute positions. GSC 3.0 also includes the GNC [9], providing an enormous improvement for galactic center observations. Further improvements on the catalogue were included on GSC 3.1 (Dec 2024), notably the inclusion of the VVV survey (Minniti et al. [14]) which improves coverage (completeness) and NIR photometry of stars in the Milky Way bulge and adjacent section of the galaxy's southern mid-plan, a crowded area, like the galactic center, of high optical extinction rendering the stars visibile only in the infrared. Note, 2MASS lacked the angular resolution needed to support JWST operations in this region.

### *4.4 OSS and ACS*

Following the initial investigation of the ACS accumulated pointing errors seen in early commissioning, OSS Build 8.4.0.4 was uploaded on March 29, 2022 to re-try ID if the Guide Star is found to be > 10" from the commanded position. This helped to reduce the number of cases where pointing errors (or drift) resulted in an incorrect Guide Star being identified. A correct GS > 10" is also rejected by this check, but in such cases re-trying would often result in a subsequent successful result as the ACS drift settles.

ACS updated its controller parameter for the FSM nominal angle to be able to start closed loop guiding from 1 arcsec to 1.2 arcsec to match the TRK box size which gives more of a chance that the visit will proceed even if there was a pointing error entering TRK. ACS also introduced an update to reset the persistency on one of their alarms to address some unsuccessful visits early in commissioning.

ACS improvements to reduce post-slew drift and improve pointing accuracy were also achieved in early commissioning. The details of these ACS efforts are beyond the scope of this paper.

OSS has completed various updates mentioned in other sections as well, related to their code to update various error paths as items were discovered during operations. Also added a count check after ACQ2 to match the 35% (now 40%) counts for BCFs that have a larger threshold in ID and ACQ1 – by the time ACQ2 is reached the non-saturated counts should match the commanded values.

## 5. SUMMARY OF CURRENT FGS PERFORMANCE ON JWST

### *5.1 Noise Equivalent Angle (NEA)*

One of the main parameters for FGS performance is its NEA (Noise Equivalent Angle) which is the standard deviation on the reported centroid positions for the GS. The requirement at launch on the FGS side was 4 mas. The measured on orbit performance summarized in Figure 15 shows the X-axis component of the NEA for different GS count rates, while in closed loop interaction with the ACS adjusting the FSM mirror based on the centroid information provided by FGS. As shown in the figure the NEA depends on the brightness of the Guide Stars and improves when the stars are brighter. The range of magnitudes used for FGS is determined by the dimmest source that can be detected giving good centroids, and the brightest one that will not oversaturate the detectors. The current magnitude range for non-

moving target operations for FGS is J = 12.5 to 18.0 for the Guide Stars – this was tuned during commissioning to confirm the conversion factor from the GSC to FGS magnitudes, and to confirm that lower and higher end.

As can be seen, the FGS performance on orbit greatly exceeds the 4 mas stability requirement with nominal operations giving values ≤ 1 mas. This is reflected on the great stability and pointing accuracy for the science targets seen on the science instruments and their ability to perform dithers and their own target acquisitions to further tune the pointing as needed for observations with great accuracy. Figure 16 shows an example of the centroid positions in X and Y reported by FGS for a visit. The standard deviation gives the NEA during that science observation.

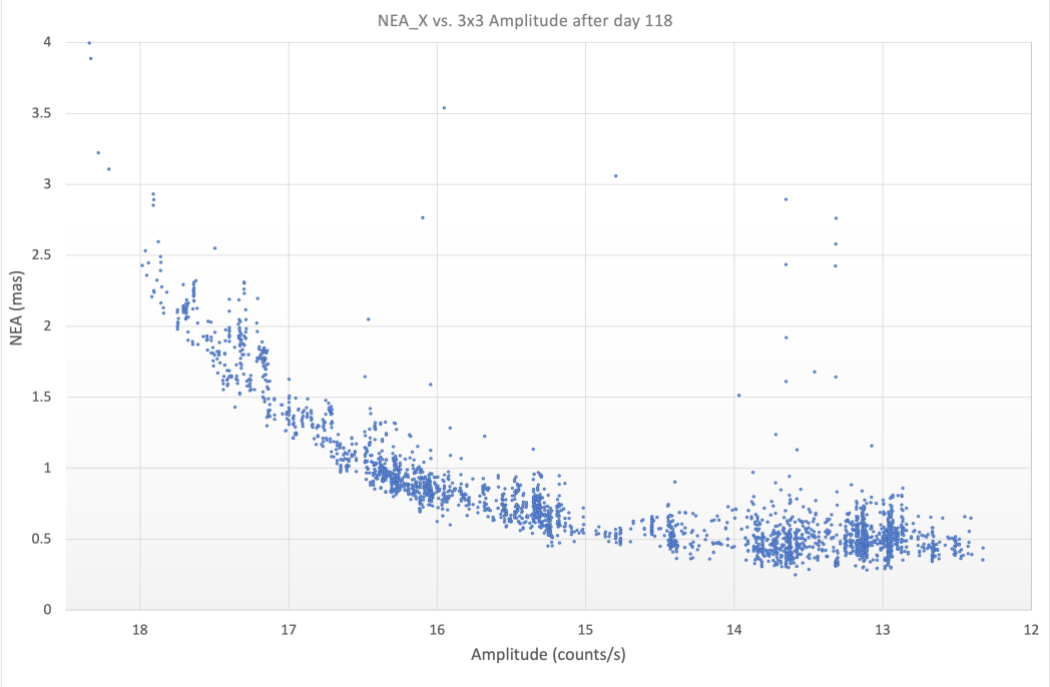


Figure 15: NEA X component distribution vs GS Count rates in 3x3 pixels box around the GS peak pixel – typical GSs used are in the ≤ 1 mas NEA

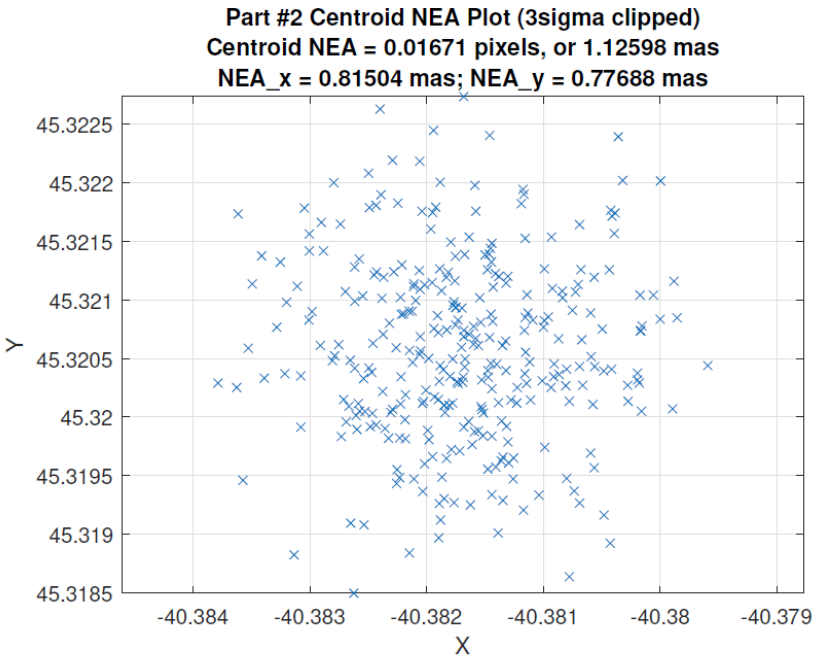


Figure 16: Typical FGS Centroid Plot with NEA < 1 mas

*5.2 Success Rate in Achieving Closed Loop with the Correct Guide Star*

Another parameter for FGS performance is the success rate in finding the correct GS for each visit and observation. Figure 17 shows the Guide Star statistics for the first 1000 days of JWST operations. As shown the FGS is successful in achieving closed loop with the correct GS ~ 95.6% of the time. Ideally a successful visit will achieve closed loop with the correct GS on the first attempt of the first GS candidate on a visit file, following the flow captured in Section 1 successfully for all activities on that visit on the first attempt (that is, passing successfully through Identification, Acquisition, Tracking, and into closed loop fine guiding with no issues or retries) – this happens ~ 82% of the time. A visit can also be successful with re-tries, meaning some of the re-try paths captured in Section 1 are followed – either a re-try in ID, or TRK or after an efficiency path entering in ACQ at science, or moving to another candidate in the visit file or an unsuccessful dither – this happens ~ 13% of the time. For these cases all science data is taken but some re-tries were needed. For ~ 4% of the visits the correct GS is not acquired or a portion of the science data is not taken due to a failure after a dither or other reason, so there is missing data for any portion of the intended science visit. For these cases visits might need to be re-scheduled to obtain all the science data once the cause of the failure is understood.

The reasons for the re-tries or for the skipped visits fall into 4 main broad categories:

- ACS/Thermal related: the GS can be too far away from commanded in ID or not be inside the ACQ or TRK box after the slew. To improve performance during early commissioning an update was added to OSS to check if FGS found the GS in ID more than 10 arcsec away from commanded position. If so a re-try would be attempted as the slew with that larger error in ID would cause the GS not to be in the ACQ

box at Science. Since that update was put in place it is very rare to not find the GS in the ACQ or TRK boxes and most of the unsuccessful visits for this reason are because the pointing error in ID is > 10 arcsec. Some small number of visits enter TRK with a larger error > 1 arcsec and ACS will not engage the closed loop in those cases. Other errors seen in early commissioning (e.g., persistency in ACS error) have been addressed during normal operations.

- Catalogue related: the star classification is not correct and it is a galaxy (lower counts than commanded) or a double star; other photometric or position errors on the catalogue; choosing a GS that is close to a very bright source like the arm of a spiral galaxy or a globular cluster or other. In early commissioning there were many duplicate entries in the catalogue that caused failures but this has been reduced in updated catalogues. Many improvements have been added (e.g., galaxy as star, counts).

- FGS related: the presence of an unmasked hot pixel not on the onboard bad pixel map – since commissioning a cadence of updating the bad pixel maps on board monthly has been implemented which has greatly reduced the chances of finding an unmasked one; a masked bad pixel that affects the counts sufficiently with the replacement algorithm so the counts do not meet the threshold for the visit file – this happens rarely and the increase of the threshold to 40% from the original 30% in early commissioning has helped to address this; count variations as the GS moves through different pixels – this point source PRNU was discovered during commissioning affecting particularly Guider 1- the increase on the counts threshold to 40% has reduced the impact; ID algorithm not finding the correct Guide Star – some of the ID parameters have been updated since commissioning optimizing performance; FG algorithm placement of the Guide Star – in some cases where there is a hot pixel or other issue the placement of the FG window is off – this is a very rare occurrence; other FGS related items.

- Other (OSS, SI target acquisition, other electronics, etc.): different items on other subsystems have been identified as JWST keeps observing and different scenarios, some very rare, are encountered. These ones are addressed when found by the different subsystems.

The FGS team established a good system during commissioning that has been refined and maintained during normal operations to identify unsuccessful visits, visits with high NEA and visits with re-tries. The team runs the analysis for all of them to understand the root cause and communicates with other subsystems as needed – e.g., notifying the GSSS not to use a particular GS if it is a double star or a galaxy; notify ACS if the pointing is off for a period of time; etc. This is a big tracking and analysis effort led by the FGS Flight Operations Team with support from FGS team members at STScI, GSFC and Canada (Honeywell and CSA) that has led to many improvements as reflected by the outstanding performance of the FGS during operations.

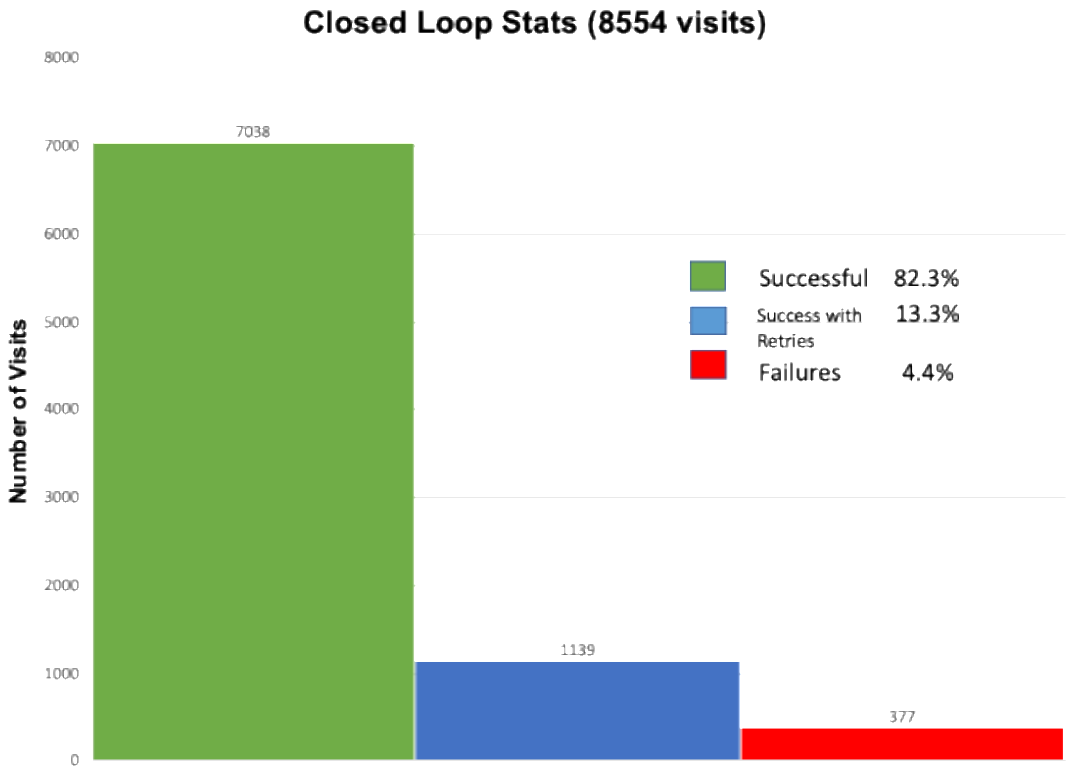


Figure 17: Summary of the Closed loop guiding statistics for the first 1000 days of JWST operations – successful GS identified ~ 95.6% of the time.

Another item monitored during operations is the coordinate frame alignment (J-frame) provided by ACS based on their on board algorithm used to determine where they think the GS is placed to where FGS finds it. A ground telemetry point is monitored that is used to flag if the ACS on board alignment has been corrupted due to incorrect information provided by FGS if the wrong GS or a hot pixel are found instead of the correct GS. It can also be caused either due to a corruption or due to drifting over time. There are processes in place that have been optimized during normal operations to reset that ACS coordinate frame on board.

### *5.3 Science Instruments Mechanisms and High Gain Antenna Effects on Guiding*

There are a number of mechanisms, both in the science instruments and the spacecraft, that are routinely activated while the FGS is in Fine Guide mode.

The disturbances can be classified as one of two types, low frequency and high frequency. In low frequency ($\lesssim 16$ Hz) disturbances, the fluctuations occur with periods greater than the rate at which centroids are being produced. In such a case, the Guide Star centroid oscillates in a decaying sinusoid, but the closed loop continues to track the Guide Star and the disturbance does not substantially impact the shape of the PSF.

By contrast, high-frequency disturbances occur on a timescale less than the exposure time of a Fine Guide Frame, and effectively blur the Guide Star PSF. The result of this blurring is a decrease in the peak amplitude of the PSF,

temporarily causing the closed loop algorithm to return "bad" centroids. However, the duration of the disturbances are brief enough that these bad centroids rarely result in a loss of lock.

The majority of guiding disturbances occur as a result of movements of the filter and pupil wheels in the science instruments. Moving the wheels in NIRCam, MIRI, and NIRSpec will produce low-frequency disturbances (~0.5 Hz) with an amplitude of 20-25 mas (~1/3 of an FGS pixel). See Figures 18 and 19 for examples of the disturbances on the measured centroids due to the mechanisms on the different SIs. The NIRISS filter and pupil wheels also produce disturbances, but because they are on the same optical bench as FGS, they also induce high-frequency modes. Note, however, that all filter wheel disturbances occur between science exposures, so do not have an impact on data quality.

Another mechanism that frequently produces disturbances in FGS guiding is the NIRSpec Micro-Shutter Array (MSA). Before many NIRSpec observations, a magnet arm moves back and forth across the MSA to open/close specific micro-shutters. This motion induces high-frequency vibrations that can result in bad centroid data for up to ~30 seconds, but generally does not result in a loss of lock. Like filter wheel movements, this occurs between exposures and has no impact on science data.

The only mechanism that regularly induces disturbances during science exposures is the High Gain Antenna (HGA). Intermittent ground station handovers require changes in HGA pointing, and these can occur at any time in a science exposure. While these disturbances can be significant (~60 mas), they are typically short enough in duration (~15 s) that the science is not significantly impacted. The FGS team is regularly monitoring the stability of individual exposures and alerts science teams of any with poor stability.

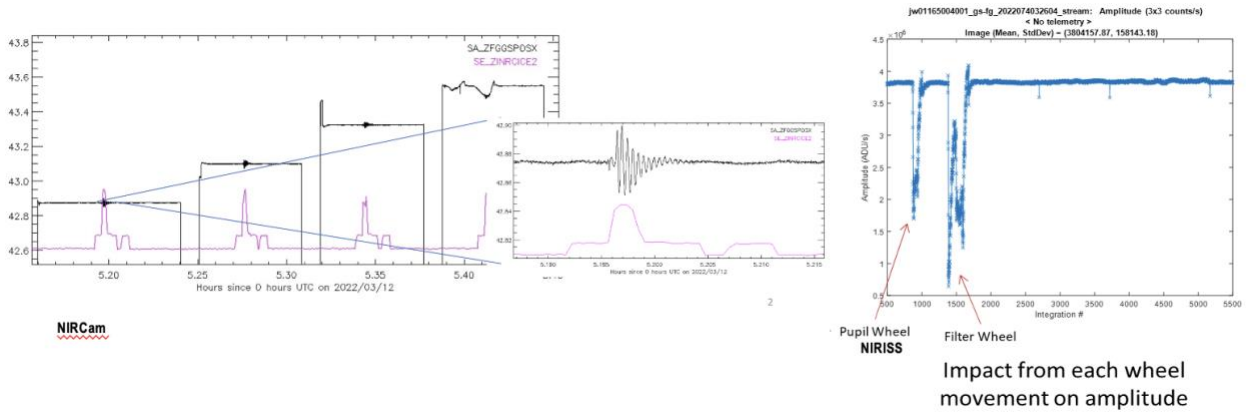


Figure 18: Examples of the disturbances seen on the FGS centroids for the wheel mechanism in NIRCam – wheel motion in red and FGS X centroids in black – and for NIRISS when its Filter and Pupil Wheels are moved – NIRISS is the instrument in the same bench as FGS.

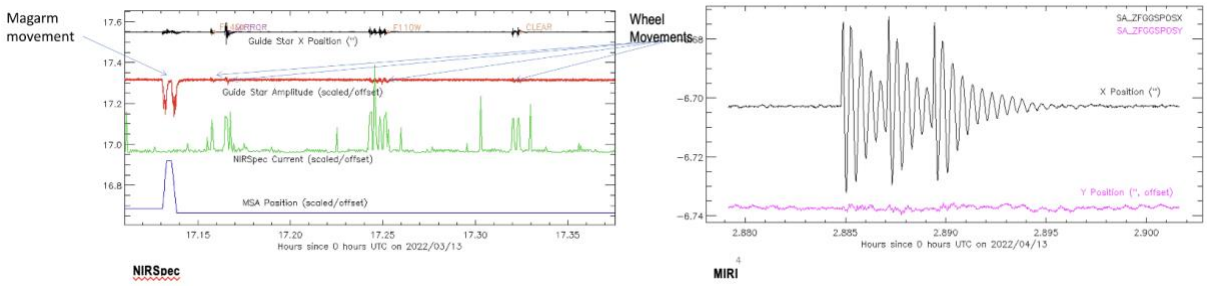


Figure 19: Examples of the disturbances seen on the FGS X centroids for the MSA magnetic arm (larger disturbance) and wheel motions in NIRSpec and the wheel in MIRI.

## 6. Other FGS Operations Activities

Covering many of the other items related to FGS commissioning and operations is beyond the scope of this paper but some items to mention at high level:

- Cosmic Rays – rate was predicted before flight and the FGS FSW algorithm takes this into account. Analysis during commissioning showed the expected rate.
- Hardware and other trending is monitored as part of normal operations - a key activity to support commissioning successfully and during normal operations to be able to monitor and analyze the FGS activities in a timely manner without impacting Observatory efficiency unduly, was to develop multiple tools for the data analysis of both images and telemetry. Many of these tools were developed prior to launch and were validated and improved with the data from cryo ground tests [e.g. 7, 15, 16, 17, 18] though significant improvements followed during commissioning and normal operations.
- On console staffing and support – the guider is often overlooked as it is seen as a science instrument but there are important differences. Most of the guider operations happen real time so any data correction needs to happen real time unlike for science where the calibrations occur once data is on the ground. Dedicated analysts were needed on shift on the FGS console to keep monitoring closed loop performance and to optimize overall guiding performance. Guiding is used for most science observations and the effort to continue improving performance on the many different types of fields is ongoing.
- Ongoing improvements as noted in this paper that continue to be addressed for operations – e.g., there is an upcoming scanning algorithm software patch to allow better calculation of star counts for bright saturated stars in ID and ACQ, etc.
- FGS as a science instrument – the guider taking the 8x8 images and producing centroids every 64 ms has been proven useful data in parallel with other science data, like for transit planet observations, and to aid in identifying mirror tilt events. Though not part of normal operations at this time the parallel guider not being used for guiding could be used to take broad band images of the sky if the data downlink bandwidth allows it. It is of interest to note that the first 'deep broadband image' of ~ 30 hours with JWST was taken with G2 during commissioning in parallel with other OTE activities – the image is captured in Figure 20.

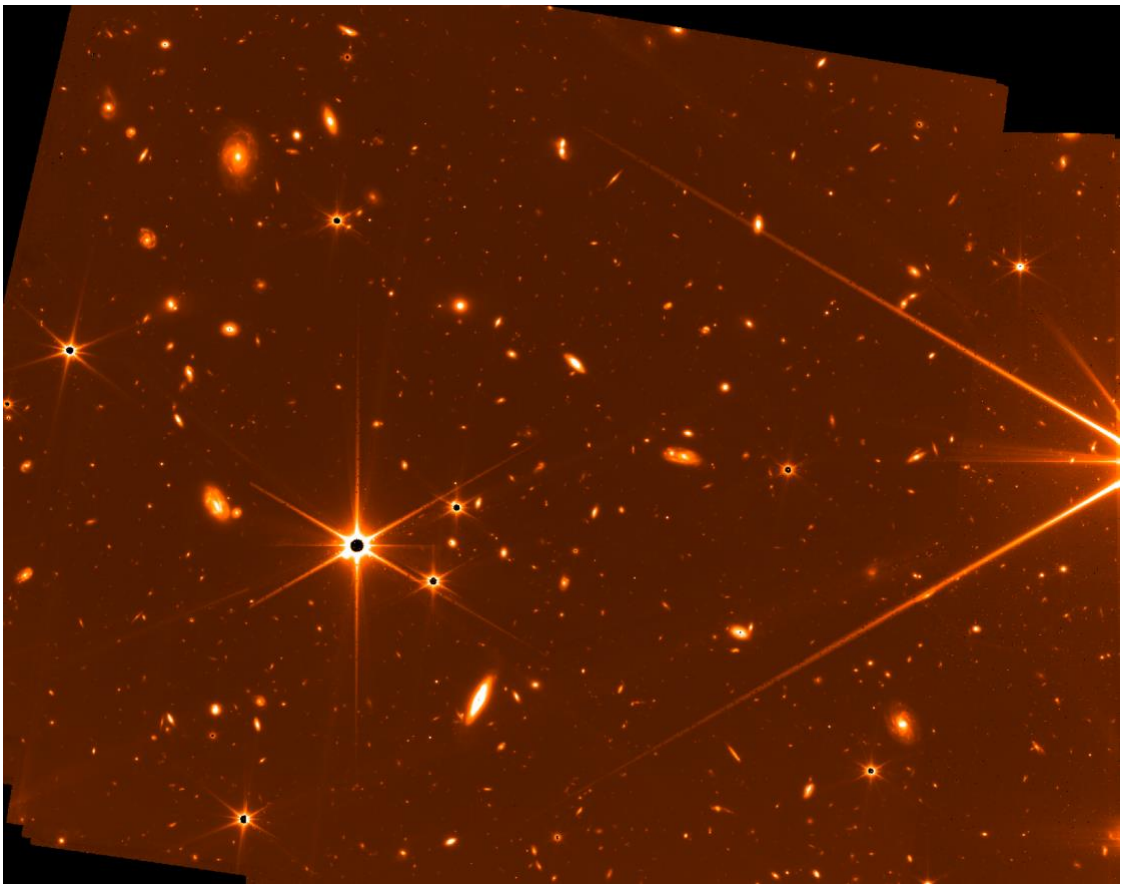

Figure 20: Guider as a broadband (0.6-5 um) imager – G2 deep ~ 30 hours full frame image.

**7. Conclusions**

This paper gives a top level summary of the FGS operations and performance for JWST. This includes what was needed to achieve closed loop during the two months for the alignment of the JWST mirrors, and all the improvements in commissioning and in normal operations to date, to achieve a remarkable ~96% success rate in achieving closed loop guiding on the correct GS with NEAs typically ≤ 1 mas for GS magnitudes above ~ J=17.5.

The FGS closed loop monitoring and analysis priorities started in commissioning and optimized for normal operations with the different tools developed, continue to provide excellent and timely information on the closed loop guiding activities and continues to be very useful in identifying possible improvements, in particular related to the Guide Star Catalogue and the FGS algorithms, as well as tracking the ACS performance for pointing.

**Acknowledgements**

The authors gratefully acknowledge all the other dedicated members that supported commissioning:

Loïc Albert, Dave Aldridge, Peter Bartosik, Peter Cameron, Steven Cuturic, Daniel Gaudreau, Fan Gong, Craig Haley, Miranda Link, Michael Maszkiewicz, Alethea Nielson, Kevin Phillips, Aidan Piwowar, Warren Soh, Michel Wander,

Andrew Wilson, Carl Wu, Michael Uzzo, Jeff Stys, Lily Liu, Dean Zak, Kyle Elliot, Keira Brooks, Shannon Osborne, Lauren Chambers.

The authors gratefully acknowledge all the other subsystems involved in commissioning, in particular the Northrop Grumman team for ACS, the Optical Telescope team at Ball Aerospace (now BAE), STScI and GSFC, and all the other leads for commissioning (Mission Operations Manager, SI leads, Timeline Coordinators, Planning & Scheduling, Science Instrument Teams).

**References**

[1] Doyon, R., Hutchings, J. B., Beaulieu, M., Albert, L., Lafrenière, D., Willott, C., Touahri, D., Rowlands, N., Maszkiewicz, M., Fullerton, A. W., Volk, K., Martel, A. R., Chayer, P. Sivaramakrishnan, A., Abraham, R., Ferrarese, L., Jayawardhana, R., Johnston, D., Meyere, M., Pipher, J. L., Sawicki, M., The JWST Fine Guidance Sensor (FGS) and Near-Infrared Imager and Slitless Spectrograph (NIRISS), 2012, Proc. SPIE 8442, 84422R.

[2] Maszkiewicz, M., Saad, K., Rowlands, N., Doyon, R. and Hutchings, J. B., JWST Fine Guidance Sensor and Near-Infrared Imager and Slitless Spectrograph, 2015, Optical Payloads for Space Missions (ed S.-E. Qian), ch35.

[3] Gardner, J. P., Mather, J. C. et al 1006 additional authors not shown), The James Webb Space Telescope Mission, 2023, PASP, Vol. 135, N. 1048.

[4] Rigby, J., Perrin, M., McElwain, M, et al. (623 additional authors not shown), The Science Performance of JWST as Characterized in Commissioning, 2023, PASP, 135, 048001.

[5] Meza, L., Tung, F., Anandakrishnan, S., Spector, V., Hyde, T., Line of Sight Stabilization of James Webb Space Telescope, 2005, 27th Annual AAS Guidance and Control Conference, AAS 05-002.

[6] Menzel, M., Davis, M., Parrish, K., Lawrence, J., Stewart, A., Cooper, J., Irish, S., Mosier, G., Levine, M., Pitman, J., Walsh, G., Maghami, P., Thomson, S., Wolldridge, E., Boucarut, R., Feinberg, L.,Turner, G., Kalia, P., Bowers, C., The Design, Verification, and Performance of the James Webb Space Telescope, 2023, PASP, 135-058002.

[7] Vila, M. B, Lambros, S. D., Diaz, D. M., Fu, H., Lee, S. S., Meza, L., Phillips, K. J., Ben del Rosario, J., Wu, C., JWST Cryo Fine Guidance Closed Loop Test Results, Proc. SPIE 10698 Space Telescopes and Instrumentation 2018: Optical, Infrared, and Millimeter Wave, 106983R.

[8] Hunter, D. G., What is it like to operate the James Webb Space Telescope?, SpaceOps2023, ID #563.

[9] Nogueras-Lara, F., Schödel, R., Gallego-Calvente, A. T., Dong, H., Gallego-Cano, E., Shahzamanian, B., Girard, J. H.V., Nishiyama, S., Najarro, F., Neumayer, N., GALACTICNUCLEUS: A high-angular-resolution $JHK_s$ imaging survey of the Galactic centre, II. First data release of the catalogue and the most detailed CMDs of the GC*, 2019, A&A 631, A20.

[10] Anderson, J., et al., The JWST Calibration Field: Absolute Astrometry and Proper Motions with GAIA and a Second HST Epoch, 2021, Technical Report JWST-STScI-007716 (Baltimore: STScI)

[11] Sohn, S. T., et al., NIRISS Commissioning Results: NIS-011(b) – NIRISS Commissioning Results: NIS-011(b) – NIRISS Geometric Distortion Calibration (NGAS CAR-374, APT 1086), 2022, JWST Technical Report JWST-STScI-008323, SM-12.

[12] McElwain, M. W., Feinberg, L. D., Perrin, M.D., Clampin, M., Mountain, M., Lallo, M.D., Lajoie, C-P, Kimble, R.A., Bowers, C. W., Stark, C. C., Action, D. S., Atkinson, C., Barinek, B., Barto, A., Basinger, S., Beck, T., Bergkoetter, D., Bluth, M., Boucarut, R.A., Brady, G.R., Brooks, K.J., Brown, B., Byard, J., Carey, L., Carrasquilla, M., Chae, D., Chaney, D., Chayer, P., Chonis, T., Chohen, L., Cole, H.J., Comau, T. M., Coon, M., Coppock, E. Coyle, L. Dean, B. H., Dziak, K. J., Eisenhower, M., Flagey, N.< Franck, R., Gallagher, B., Gilman, L., Glassman, T., Green, J. J., Grieco, J., Haase, S., Hadjimichael, T. J., Hagopian, J. G., Hahn, W. G., Hartig, G. F., Havey, K. A., Hayden, W. L., Hellkson, R., Hicks, B., Holfeltz, S. T., Howard, J. M., Huguet, J. A., Jahne, B., Johnson, L. A., Johnston, J. D., Jurling, A. S., Kegley, J.R., Kennard, S., Keski-Kuha, R. A., Knight, J. S., Kulp, B. A., Levi, J. S., Levine, M. B., Lightsey, P. Luetgens, R. A., Mather, J. C., Matthews, G. W., McKay, A. G., Mehalick, K. I., Meléndez, M., Mosier, G. E. Murphy, J., Nelan, E.P., Niedneer, M. B., Nol, D. M., Ohara, C. M., Ohl, R. G., Olczak, E., Osborne, S.B., Park, S., Perrygo, C., Pueyo, L., Redding, D. C., Regan, M. W., Reynolds, P., Rifelli, R., Rigby, J.R., Sabatke, D., Saif, B.N., Scorse, T. R., Seo, B0J, Shi, F., Sigrist, N., Smith, K. Smith, J.S., Smith, E.C., Soh, S. T., Stahl, H. P., Telfer, R., Terlecki, T., Texter, S.C., Van Buren, D, Van Campen, J. M., Vila, B., Voyton, M. F., Wlakdman, M., Walker, C. B., Weiser, N., Wells, C., West, G., Whitman, T. L., Wolf, E., Zielinski, T. P., The James Webb Space Telescope Mission: Optical Telescope Element Design, Development and Performance, 2023_PASP, 135-058001.

[13] Warner, G., Barringer, B., Bond, N., Chayer, P., DiFelice, A., Dupuis, J., Holfeltz, S., Lambros, S. D., Marrione, A., Moller, C. D., Nelan, E., Rowlands, N., Shon, S.T., Vila, M. B., Yeates, J., Zhou, J., 2025, JWST Fine Guidance Sensor Optimizations and Improvements since Launch, SpaceOps 2025, Paper ID#228.

[14] Minniti D., Lucas P.W., Emerson J., Saito R., Hempel M., Pietrukowicz, Ahumada A.V., Alonso M.V., Alonso-Garcia J., July 2010, VISTA Variables in the Via Lactea (VVV): The public ESO near-IR variability survey of the Milky Way, New Astronomy, 15 (10): 433–443.

[15] Kimble, R. A, Vila, M.B, Van Campen, J. M., Birkmann, S. M., Comber, B. J., Fatig, C. C., Glasse, A. C. H., Glazer, S. D., Kelly, D. M., Mann, S. D., Martel, A. R., Novo-Gradac, K. J., Ohl, R. G., Penanen, K. I., Rohrback, S. O., Sullivan, J. F., Zak, D., Zhou, J., Cryo-vacuum testing of the JWST integrated science instrument module (ISIM), 2016, Proc. SPIE 9904.

[16] Rowlands, N., Beaton, A., Chayer, P., Haley, C., Midwinter, C., Volk, K., Warner, G., Zhou, J., Updated cryogenic performance test results for the flight model JWST fine guidance sensor, 2016, Proc. SPIE 9904, Space Telescopes and Instrumentation 2016: Optical, Infrared, and Millimeter Wave.

[17] Rowlands, N., Delamer, S., Haley, C., Harpell, E., Vila, M. B., Warner, G., Zhou, J., Cryogenic performance test results for the flight model JWST fine guidance sensor, 2012, SPIE, 8442-130.

[18] Vila, M. B., Rowlands, N., Desaulniers, D-L., Evans., C., JWST Fine Guidance Sensor Performance Analysis, 2008 CASI ASTRO 2008, Proceedings, 62.